

A Layman's Guide to Two Loops

Giampiero PASSARINO

Dipartimento di Fisica Teorica, Università di Torino, Italy
INFN, Sezione di Torino, Italy



Freiburg, September 2009



Outlines

(1, 2, 3)

- 1 *In this lecture the building blocks for the two-loop renormalization of the Standard Model will be introduced Two-loop Ward-Slavnov-Taylor identities and the complete set of counterterms needed for two-loop renormalization will be discussed.*
- 2 *In this lecture a renormalization scheme will be introduced, connecting the renormalized quantities to an input parameter set of (pseudo-)experimental data.*
- 3 *In this lecture the set of techniques needed to compute decay rates at the two-loop level will be derived. The main emphasis of the lecture will be on the two Standard Model decays $H \rightarrow \gamma\gamma$ and $H \rightarrow gg$.*



Outlines

(1, 2, 3,)

- 1** *In this lecture the building blocks for the two-loop renormalization of the Standard Model will be introduced Two-loop Ward-Slavnov-Taylor identities and the complete set of counterterms needed for two-loop renormalization will be discussed.* ▶ L1
- In this lecture a renormalization scheme will be introduced, connecting the renormalized quantities to an input parameter set of (pseudo-)experimental data.* ▶ L2
- In this lecture the set of techniques needed to compute decay rates at the two-loop level will be derived. The main emphasis of the lecture will be on the two Standard Model decays $H \rightarrow \gamma\gamma$ and $H \rightarrow gg$.*

▶ L3



Outlines

(1, 2, 3,)

- 1 *In this lecture the building blocks for the two-loop renormalization of the Standard Model will be introduced Two-loop Ward-Slavnov-Taylor identities and the complete set of counterterms needed for two-loop renormalization will be discussed.* ▶ L1
- 2 *In this lecture a renormalization scheme will be introduced, connecting the renormalized quantities to an input parameter set of (pseudo-)experimental data.* ▶ L2
- 3 *In this lecture the set of techniques needed to compute decay rates at the two-loop level will be derived. The main emphasis of the lecture will be on the two Standard Model decays $H \rightarrow \gamma\gamma$ and $H \rightarrow gg$.*

▶ L3



Outlines

(1, 2, 3,)

- 1 *In this lecture the building blocks for the two-loop renormalization of the Standard Model will be introduced Two-loop Ward-Slavnov-Taylor identities and the complete set of counterterms needed for two-loop renormalization will be discussed.* ▶ L1
- 2 *In this lecture a renormalization scheme will be introduced, connecting the renormalized quantities to an input parameter set of (pseudo-)experimental data.* ▶ L2
- 3 *In this lecture the set of techniques needed to compute decay rates at the two-loop level will be derived. The main emphasis of the lecture will be on the two Standard Model decays $H \rightarrow \gamma\gamma$ and $H \rightarrow gg$.*

▶ L3



Part I

Lecture I



Basics

The minimal Higgs sector of the SM is provided by the Lagrangian

$$\mathcal{L}_S = -(D_\mu K)^\dagger (D_\mu K) - \mu^2 K^\dagger K - (\lambda/2)(K^\dagger K)^2, \quad (1)$$

where the covariant derivative is given by

$$D_\mu K = \left(\partial_\mu - \frac{i}{2} g B_\mu^a \tau^a - \frac{i}{2} g' B_\mu^0 \right) K, \quad (2)$$

$g'/g = -\sin\theta/\cos\theta$, θ is the weak mixing angle, τ^a are the standard Pauli matrices, B_μ^a is a triplet of vector gauge bosons and B_μ^0 a singlet. For the theory to be stable we must require $\lambda > 0$. We choose $\mu^2 < 0$ in order to have SSB. The scalar field in the minimal realization of the SM is

$$K = \frac{1}{\sqrt{2}} \begin{pmatrix} \zeta + i\phi_0 \\ -\phi_2 + i\phi_1 \end{pmatrix}, \quad (3)$$

where ζ and the Higgs-Kibble fields ϕ_0 , ϕ_1 and ϕ_2 are real. For $\mu^2 < 0$ we have SSB, $\langle K \rangle_0 \neq 0$. In particular, we choose $\zeta + i\phi_0$ to be the component of K to develop the non-zero VEV, and we set $\langle \phi_0 \rangle_0 = 0$ and $\langle \zeta \rangle_0 \neq 0$. We then introduce the (physical) Higgs fields as $H = \zeta - v$. The parameter v is not a new parameter of the model; its value must be fixed by the requirement that $\langle H \rangle_0 = 0$ (i.e. $\langle K \rangle_0 = (1/\sqrt{2})(v, 0)$), so that the vacuum doesn't absorb/create Higgs particles.



Tadpoles do not depend on any particular scale other than their internal mass, and cancel in any renormalized self-energy. However, they play an essential role in proving the gauge invariance of all the building blocks of the theory.

- In order to exploit this option, we will now consider a strategy to set the Higgs VEV to zero.

We will define the new bare parameters M' (the W boson mass), M'_H (the mass of the physical Higgs particle) and β_t (the tadpole constant) according to the following “ β_t scheme”:

$$\left\{ \begin{array}{l} M'(1 + \beta_t) = gv/2 \\ (M'_H)^2 = \lambda (2M'/g)^2 \\ 0 = \mu^2 + \frac{\lambda}{2} (2M'/g)^2 \end{array} \right. \implies \left\{ \begin{array}{l} v = 2M'(1 + \beta_t)/g \\ \lambda = (gM'_H/2M')^2 \\ \mu^2 = -\frac{1}{2}(M'_H)^2 \end{array} \right. \quad (4)$$



The new set of bare parameters is therefore g, g', M', M'_H and β_t . Remember that β_t is not an independent parameter and it appears in the Higgs doublet K via $\zeta = H + v$, with $v = 2M'(1 + \beta_t)/g$. As a consequence, all three terms of the Lagrangian \mathcal{L}_S in Eq.(1) depend on this parameter. In particular, the interaction part of \mathcal{L}_S becomes

$$\mathcal{L}'_S = -\mu^2 K^\dagger K - (\lambda/2)(K^\dagger K)^2 \quad (5)$$

$$\begin{aligned} &= (1 + \beta_t)^2 \left(1 - \beta_t(2 + \beta_t)\right) \frac{M_H'^2 M'^2}{2g^2} - \beta_t(\beta_t + 1)(\beta_t + 2) \frac{M_H'^2 M'}{g} H \\ &\quad - \frac{1}{2} M_H'^2 H^2 - \frac{1}{4} M_H'^2 \beta_t(\beta_t + 2) \left(3H^2 + \phi_0^2 + 2\phi_+\phi_-\right) \\ &\quad - g(1 + \beta_t) \frac{M_H'^2}{4M'} H \left(H^2 + \phi_0^2 + 2\phi_+\phi_-\right) \\ &\quad - g^2 \frac{M_H'^2}{32M'^2} \left(H^2 + \phi_0^2 + 2\phi_+\phi_-\right)^2, \end{aligned} \quad (6)$$



while the term of \mathcal{L}_S involving $-(D_\mu K)^\dagger (D_\mu K)$, yields a (lengthy) β_t -independent expression, plus the following terms containing β_t :

$$\begin{aligned}
 \beta_t \times & \left[i g s_\theta M' (\phi^- W_\mu^+ - \phi^+ W_\mu^-) (A_\mu - \frac{s_\theta}{c_\theta} Z_\mu) \right. \\
 & - \frac{g M'}{2} H (2 W_\mu^+ W_\mu^- + \frac{Z_\mu Z_\mu}{c_\theta^2}) \\
 & - \frac{M'^2}{2} (\beta_t + 2) (2 W_\mu^+ W_\mu^- + \frac{Z_\mu Z_\mu}{c_\theta^2}) \\
 & \left. + \frac{M'}{c_\theta} Z_\mu \partial_\mu \phi_0 + M' W_\mu^+ \partial_\mu \phi_- + M' W_\mu^- \partial_\mu \phi_+ \right], \tag{7}
 \end{aligned}$$

where, as usual, $W_\mu^\pm = (B_\mu^1 \mp i B_\mu^2) / \sqrt{2}$, and

$$\begin{pmatrix} Z_\mu \\ A_\mu \end{pmatrix} = \begin{pmatrix} c_\theta & -s_\theta \\ s_\theta & c_\theta \end{pmatrix} \begin{pmatrix} B_\mu^3 \\ B_\mu^0 \end{pmatrix}. \tag{8}$$



Where else, in the SM Lagrangian, does the parameter β_t appear? Wherever v does — as it can be readily seen from Eq.(4). Let us now quickly discuss the other sectors of the SM: Yang–Mills, fermionic, Faddeev–Popov (FP) and gauge-fixing. The pure Yang–Mills Lagrangian obviously contains no β_t terms.

The gauge-fixing part of the Lagrangian, \mathcal{L}_{gf} , cancels in the R_ξ gauges the gauge–scalar mixing terms $Z-\phi_0$ and $W^\pm-\phi^\pm$ contained in the scalar Lagrangian \mathcal{L}_S . These terms are proportional to $gv/2$, i.e., to $M'(1 + \beta_t)$ in the β_t scheme. The gauge-fixing Lagrangian \mathcal{L}_{gf} is a matter of choice: we adopt the usual definition

$$\mathcal{L}_{gf} = -C_+C_- - \frac{1}{2}C_Z^2 - \frac{1}{2}C_A^2, \quad (9)$$

with

$$C_A = -\frac{1}{\xi_A}\partial_\mu A_\mu, \quad C_Z = -\frac{1}{\xi_Z}\partial_\mu Z_\mu + \xi_Z \frac{M'}{c_\theta}\phi_0, \quad C_\pm = -\frac{1}{\xi_W}\partial_\mu W_\mu^\pm + \xi_W M'\phi_\pm \quad (10)$$



(note: no β_t terms), thus canceling the \mathcal{L}_S g -independent gauge–scalar mixing terms proportional to M' , but not those proportional to $M'\beta_t$ (appearing at the end of Eq.(7)), which are of $\mathcal{O}(g^2)$.

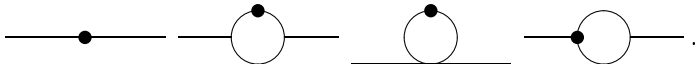
Alternatively, one could choose $M'(1 + \beta_t)$ instead of M' in Eq.(10), thus canceling all \mathcal{L}_S gauge–scalar mixing terms, both proportional to M' and $M'\beta_t$, but introducing then new two-leg β_t vertices. We will not follow this latter approach.

- Of course it is only a matter of choice, but the explicit form of \mathcal{L}_{gf} determines the FP ghost Lagrangian.

The parameter β_t shows up also in the FP ghost sector. The FP Lagrangian depends on the gauge variations of the chosen gauge-fixing functions \mathcal{C}_A , \mathcal{C}_Z and \mathcal{C}_\pm .



In the β_t scheme we have (many) two- and three-leg β_t vertices containing also non-scalar fields. Note that three-leg β_t vertices introduce a fourth irreducible topology for $\mathcal{O}(g^4)$ self-energy diagrams containing β_t vertices, namely:



Define $\beta_t = \beta_{t_0} + \beta_{t_1} g^2 + \beta_{t_2} g^4 + \dots$. We will now fix the parameter β_t such that the VEV of the Higgs field H remains zero order by order in perturbation theory. At the lowest order, the only diagram contributing to $\langle H \rangle_0$ is the one depicted in Eq.(15),

$$H \text{ --- } \bullet \quad (15)$$

which originates from the term in \mathcal{L}'_S linear in H , $-\beta_t(\beta_t + 1)(\beta_t + 2)(M_H^2 M' / g)H$. Therefore, at the lowest order we can simply set $\beta_t = 0$, i.e. $\beta_{t_0} = 0$. Up to one loop, the diagrams T'_0 and T'_1 contributing to the Higgs VEV are

$$T'_0 : \text{ --- } \bullet + T'_1 : \text{ --- } \bigcirc \quad (16)$$

so that

$$\beta_{t_1} = \frac{1}{(2\pi)^4 i} \left(\frac{T'_1}{2M' g M_H^2} \right). \quad (17)$$



Up to terms of $\mathcal{O}(g^3)$, $\langle H \rangle_0$ gets contributions from the following diagrams:

$$T'_0: \text{---} \bullet \quad (1) \quad +$$

$$T'_1: \text{---} \bigcirc \quad (1/2) \quad +$$

$$T'_2: \text{---} \bigcirc \quad (1/6) \quad + \quad \text{---} \bigcirc \quad (1/4) \quad + \quad \text{---} \bigcirc \bigcirc \quad (1/4) \quad +$$

$$T'_3: \text{---} \bigcirc \bullet \quad (1/2) \quad + \quad \text{---} \bullet \bigcirc \quad (1/2),$$

plus reducible diagrams (analogous to those appearing in T_4 – T_7 of section 2.4) which add up to zero because of our choice for β_{t_0} and β_{t_1} . Note the new diagrams in T'_3 , with three-leg β_t vertices, not present in the β_h case (T_3). The parameter β_{t_2} can be set in the usual manner, requiring

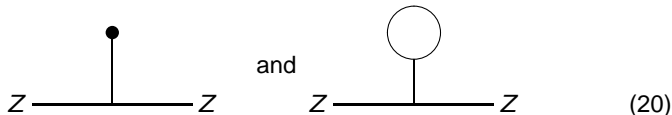
$$\sum_{i=0}^3 T'_i = 0, \quad \Rightarrow \quad \beta_{t_2} = \frac{1}{(2\pi)^{4j}} \left(\frac{T'_2 + T'_3}{2M'g^3M_H^{j/2}} \right) - \frac{3}{2}\beta_{t_1}^2. \quad (18)$$



Consider the (doubly-contracted) WST identity relating the Z self-energy $\Pi_{\mu\nu,ZZ}(p)$, the ϕ_0 self-energy $\Pi_{\phi_0\phi_0}(p)$, and the $Z-\phi_0$ transition $\Pi_{\mu,Z\phi_0}(p)$:

$$p_\mu p_\nu \Pi_{\mu\nu,ZZ}(p) + M_0^2 \Pi_{\phi_0\phi_0}(p) + 2ip_\mu M_0 \Pi_{\mu,Z\phi_0}(p) = 0. \quad (19)$$

Each of the three terms in Eq.(19) contains contributions from the tadpole diagrams, but they add up to zero, within each term. For example, at the one-loop level, the first term in Eq.(19) contains the tadpole diagrams



$$\text{Z} \text{---} \text{---} \text{Z} \quad \text{and} \quad \text{Z} \text{---} \text{---} \text{Z} \quad (20)$$

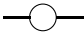


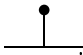
which cancel each other.



In the β_t scheme, all three terms of Eq.(19) contain the two-leg β_t vertices already at the one-loop level. Similar comments are valid for the WST identity involving the W self-energy.

Concerning renormalization, the constraints imposed on β_t in the previous sections are the renormalization conditions to insure that $\langle 0|H|0\rangle = 0$, also in the presence of radiative corrections. In particular, the renormalized β_t parameter is $\beta_t^{(R)} = \beta_t + \delta\beta_t = 0$. The equivalent of Eq. (4) for the renormalized parameters is just the same equation with the tadpole constants set to zero.

In the β_t scheme, the one-loop renormalization of the W and Z masses involves the diagrams

(a)  (c)  (b)  (d)  (21)

Both (a) and (b) diagrams are gauge-dependent, their sum is gauge-independent on-shell, and the β_t tadpole (d) is chosen to cancel (b). But, the mass counterterm is now gauge-independent, as it contains both (a) and the two-leg β_t vertex diagram (c).



Diagonalization of the neutral sector

The $Z-\gamma$ transition in the SM does not vanish at zero squared momentum transfer. Although this fact does not pose any serious problem, not even for the renormalization of the electric charge, it is preferable to use an alternative strategy. Consider the new $SU(2)$ coupling constant \bar{g} , the new mixing angle $\bar{\theta}$ and the new W mass \bar{M} in the β_h scheme:

$$\begin{aligned} g &= \bar{g}(1 + \Gamma) & g' &= -(\sin \bar{\theta} / \cos \bar{\theta}) \bar{g} \\ v &= 2\bar{M}/\bar{g} & \lambda &= (\bar{g}M_H/2\bar{M})^2 & \mu^2 &= \beta_h - \frac{1}{2}M_H^2 \end{aligned} \quad (22)$$

(note: $g \sin \theta / \cos \theta = \bar{g} \sin \bar{\theta} / \cos \bar{\theta}$), where $\Gamma = \Gamma_1 \bar{g}^2 + \Gamma_2 \bar{g}^4 + \dots$ is a new parameter yet to be specified. This change of parameters entails new \bar{A}_μ and \bar{Z}_μ fields related to B_μ^3 and B_μ^0 by

$$\begin{pmatrix} \bar{Z}_\mu \\ \bar{A}_\mu \end{pmatrix} = \begin{pmatrix} \cos \bar{\theta} & -\sin \bar{\theta} \\ \sin \bar{\theta} & \cos \bar{\theta} \end{pmatrix} \begin{pmatrix} B_\mu^3 \\ B_\mu^0 \end{pmatrix}. \quad (23)$$



The replacement $g \rightarrow \bar{g}(1 + \Gamma)$ introduces in the SM Lagrangian several terms containing the new parameter Γ . In our approach Γ is fixed, order-by-order, by requiring that the $Z-\gamma$ transition is zero at $p^2 = 0$ in the $\xi = 1$ gauge. Let us take a close look at these ‘ Γ terms’ in each sector of the SM.

- The pure Yang–Mills Lagrangian

$$\mathcal{L}_{YM} = -\frac{1}{4}F_{\mu\nu}^a F_{\mu\nu}^a - \frac{1}{4}F_{\mu\nu}^0 F_{\mu\nu}^0, \quad (24)$$

with $F_{\mu\nu}^a = \partial_\mu B_\nu^a - \partial_\nu B_\mu^a + g\epsilon^{abc}B_\mu^b B_\nu^c$ and $F_{\mu\nu}^0 = \partial_\mu B_\nu^0 - \partial_\nu B_\mu^0$, contains the following new Γ terms when we replace g by $\bar{g}(1 + \Gamma)$:

$$\begin{aligned} \Delta\mathcal{L}_{YM} = & i\bar{g}\Gamma\bar{c}_\theta [\partial_\nu\bar{Z}_\mu (W_\mu^+ W_\nu^- - W_\nu^+ W_\mu^-) - \bar{Z}_\nu (W_\mu^+ \partial_\nu W_\mu^- - W_\mu^- \partial_\nu W_\mu^+) + \\ & + \bar{Z}_\mu (W_\nu^+ \partial_\nu W_\mu^- - W_\nu^- \partial_\nu W_\mu^+)] - i\bar{g}\Gamma\bar{s}_\theta [\partial_\nu\bar{A}_\mu (W_\mu^+ W_\nu^- - W_\nu^+ W_\mu^-) \\ & - \bar{A}_\nu (W_\mu^+ \partial_\nu W_\mu^- - W_\mu^- \partial_\nu W_\mu^+) + \bar{A}_\mu (W_\nu^+ \partial_\nu W_\mu^- - W_\nu^- \partial_\nu W_\mu^+)] \\ & + \bar{g}^2\Gamma(2 + \Gamma) \left[\frac{1}{2}(W_\mu^+ W_\nu^- W_\mu^+ W_\nu^- - W_\mu^+ W_\mu^- W_\nu^+ W_\nu^-) \right. \\ & + \bar{c}_\theta^2 (\bar{Z}_\mu W_\mu^+ \bar{Z}_\nu W_\nu^- - \bar{Z}_\mu \bar{Z}_\mu W_\nu^+ W_\nu^-) + \bar{s}_\theta^2 (\bar{A}_\mu W_\mu^+ \bar{A}_\nu W_\nu^- - \bar{A}_\mu \bar{A}_\mu W_\nu^+ W_\nu^-) \\ & \left. + \bar{s}_\theta \bar{c}_\theta (\bar{A}_\mu \bar{Z}_\nu (W_\mu^+ W_\nu^- + W_\nu^+ W_\mu^-) - 2\bar{A}_\mu \bar{Z}_\mu W_\nu^+ W_\nu^-) \right], \quad (25) \end{aligned}$$

where $\bar{s}_\theta = \sin \bar{\theta}$ and $\bar{c}_\theta = \cos \bar{\theta}$. As these terms are of $\mathcal{O}(\bar{g}^3)$ or $\mathcal{O}(\bar{g}^4)$, they do not contribute to the calculation of self-energies at the one-loop level, but they do beyond it.



New coupling constant in the β_t scheme

The β_t scheme equations are the following

$$\begin{aligned} g &= \bar{g}(1 + \Gamma) & g' &= -(\sin \bar{\theta} / \cos \bar{\theta}) \bar{g} \\ v &= 2\bar{M}'(1 + \beta_t) / \bar{g} & \lambda &= (\bar{g}M'_H / 2\bar{M}')^2 & \mu^2 &= -\frac{1}{2}(M'_H)^2. \end{aligned} \quad (26)$$

(Note: $g \sin \theta / \cos \theta = \bar{g} \sin \bar{\theta} / \cos \bar{\theta}$.) The new fields \bar{A}_μ and \bar{Z}_μ are related to B_μ^3 and B_μ^0 by Eq.(23). Thus, we obtain the following results:



- The replacement $g \rightarrow \bar{g}(1 + \Gamma)$ in the pure Yang–Mills sector introduces new Γ vertices collected in $\Delta\mathcal{L}_{YM}$, which does not depend on the parameters of the β_t schemes. $\Delta\mathcal{L}_{YM}$ will not be given here.
- The new Γ terms introduced in \mathcal{L}_S by eqs. (26) can be arranged once again in the three classes

$$\Delta\mathcal{L}_{S,t} = \Delta\mathcal{L}_{S,t}^{(n_f=2)} + \Delta\mathcal{L}_{S,t}^{(n_f=3)} + \Delta\mathcal{L}_{S,t}^{(n_f=4)}, \quad (27)$$

according to the number of fields appearing in the Γ terms. The explicit expression for $\Delta\mathcal{L}_{S,t}^{(2)}$ is, up to terms of $\mathcal{O}(\bar{g}^4)$,



$$\begin{aligned}
\Delta \mathcal{L}_{S,t}^{(n_f=2)} = \bar{M}' \Gamma & \left[-\frac{1}{2} \bar{M}' \bar{s}_\theta^2 \Gamma \bar{A}_\mu \bar{A}_\mu - \frac{1}{2} \bar{M}' (2 + \Gamma \bar{c}_\theta^2 + 4\beta_t) \bar{Z}_\mu^0 \bar{Z}_\mu^0 \right. \\
& - \bar{M}' \frac{\bar{s}_\theta}{\bar{c}_\theta} (1 + \Gamma \bar{c}_\theta^2 + 2\beta_t) \bar{A}_\mu \bar{Z}_\mu^0 + \partial_\mu \phi_0 (\bar{s}_\theta \bar{A}_\mu + \bar{c}_\theta \bar{Z}_\mu^0) (1 + \beta_t) \\
& \left. - \bar{M}' (2 + \Gamma + 4\beta_t) W_\mu^+ W_\mu^- + (W_\mu^- \partial_\mu \phi^+ + W_\mu^+ \partial_\mu \phi^-) (1 + \beta_t) \right] \quad (28)
\end{aligned}$$

with $\bar{s}_\theta = \sin \bar{\theta}$ and $\bar{c}_\theta = \cos \bar{\theta}$, etc.



- Our recipe for gauge-fixing is the same as in the previous sections: **we choose the R_ξ gauge \mathcal{L}_{gf} to cancel the zeroth order (in \bar{g}) gauge–scalar mixing terms introduced by \mathcal{L}_S** , but not those of higher orders. Here, this prescription is realized by \mathcal{L}_{gf} with

$$C_A = -\frac{1}{\xi_A} \partial_\mu \bar{A}_\mu, \quad C_Z = -\frac{1}{\xi_Z} \partial_\mu \bar{Z}_\mu^0 + \xi_Z \frac{\bar{M}'}{\bar{c}} \phi_0, \quad C_\pm = -\frac{1}{\xi_W} \partial_\mu W_\mu^\pm + \xi_W \bar{M}' \phi_\pm, \quad (29)$$

clearly Γ -independent.



The **new Γ terms** of the **FP ghost Lagrangian** in the β_t scheme are:

$$\Delta\mathcal{L}_{FP,t} = \Delta\mathcal{L}_{FP,t}^{(n_f=2)} + \Delta\mathcal{L}_{FP,t}^{(n_f=3)}, \quad (30)$$

where the two-field terms are

$$\Delta\mathcal{L}_{FP,t}^{(n_f=2)} = - (1 + \beta_t) \Gamma \bar{M}'^2 \left[\xi_Z \bar{X}_Z \left(X_Z + \frac{\bar{S}_\theta}{\bar{C}_\theta} X_A \right) + \xi_W \left(\bar{X}_+ X_+ + \bar{X}_- X_- \right) \right], \quad (31)$$

Like in the scalar sector, the **Γ and β_t factors** are entangled.



We conclude this analysis with the fermionic sector

. As in the Yang–Mills case, the fermion – gauge boson Lagrangian \mathcal{L}_{fG} does not depend on the parameters of the β_t scheme. Its expression in terms of the new coupling constant \bar{g} contains new Γ terms.

The neutral sector re-diagonalization

induces no Γ terms in the fermion–scalar Lagrangian \mathcal{L}_{fS} , which contains, however, the β_t vertices (the ratio M'/g is now replaced by the identical ratio \bar{M}'/\bar{g}).



The Γ - β_t mixing

A comment on the presence of β_t factors in the new Γ vertices is now appropriate. Consider the scalar Lagrangian \mathcal{L}_S . The interaction part of \mathcal{L}_S ,

$$\mathcal{L}_S^I = -\mu^2 K^\dagger K - (\lambda/2)(K^\dagger K)^2,$$

does not induce Γ terms. On the other hand, \mathcal{L}_S^I gives rise to β_t terms: as $M'/g = \bar{M}'/\bar{g}$, these β_t terms are simply expressed in terms of \bar{M}'/\bar{g} instead of M'/g .

The derivative part of the scalar Lagrangian,

$$-(D_\mu K)^\dagger (D_\mu K),$$

induces both Γ and β_t vertices, plus mixed ones which we still call Γ vertices (see the β_t factors in the two-leg Γ terms of $\Delta\mathcal{L}_{S,t}^{(n_f=2)}$).



It works like this: first, we replace $g \rightarrow \bar{g}(1 + \Gamma)$ and $g' \rightarrow -\bar{g}(\bar{S}_\theta/\bar{c}_\theta)$ in $-(D_\mu K)^\dagger(D_\mu K)$, splitting the result in two classes of terms, both written in terms of \bar{g} , with or without Γ .

Then we substitute in both classes $v \rightarrow 2\bar{M}'(1 + \beta_t)/\bar{g}$: the class containing Γ is, up to terms of $\mathcal{O}(\bar{g}^4)$, $\Delta\mathcal{L}_{S,t}$ [Eq.(27)], and includes also β_t factors, while the class free of Γ has the same β_t vertices as Eq.(7) with g, θ, M', A_μ and Z_μ replaced by $\bar{g}, \bar{\theta}, \bar{M}', \bar{A}_\mu$ and \bar{Z}_μ^0 . The upshot is that you need both the results for the new Γ vertices derived in the previous section 1 (containing β_t), and the expressions for the β_t terms.

The Γ and β_t terms of the Faddeev–Popov sector are intertwined just as in the case of the scalar Lagrangian.



WSTI for two-loop gauge boson self-energies

WSTI

The purpose of this section is to discuss in detail the structure of the (doubly-contracted) *Ward-Slavnov-Taylor identities* (WSTI) for the *two-loop gauge boson self-energies in the Standard Model*, focusing in particular on the role played by the reducible diagrams. This analysis is performed in the 't Hooft–Feynman gauge.



Definitions and WST identities

Let Π_{ij} be the sum of all diagrams (both one-particle reducible and irreducible) with two external boson fields, i and j , to all orders in perturbation theory (as usual, the external Born propagators are not to be included in the expression for Π_{ij})

$$\Pi_{ij} = \sum_{n=1}^{\infty} \frac{g^{2n}}{(16\pi^2)^n} \Pi_{ij}^{(n)}. \quad (32)$$

In the subscripts of the quantities $\Pi_{ij}^{(n)}$ we will also explicitly indicate, when necessary, the appropriate Lorentz indices with Greek letters. At each order in the perturbative expansion it is convenient to **make explicit the tensor structure** of these functions by employing the following definitions:



$$\Pi_{\mu\nu, VV}^{(n)} = D_{VV}^{(n)} \delta_{\mu\nu} + P_{VV}^{(n)} p_\mu p_\nu \quad \Pi_{\mu, VS}^{(n)} = -ip_\mu M_S G_{VS}^{(n)} \quad \Pi_{SS}^{(n)} = R_{SS}^{(n)}, \quad (33)$$

where the subscripts **V** and **S** indicate **vector** and **scalar** fields, M_S is the mass of the Nambu–Goldstone scalar S , and p is the incoming momentum of the vector boson (note: $\Pi_{\mu, SV}^{(n)} = -\Pi_{\mu, VS}^{(n)}$).

The quantities D_{ij} , P_{ij} , G_{ij} , and R_{ij} depend only on the squared four-momentum and are symmetric in i and j . Furthermore, D and R have the dimensions of a mass squared, while G and P are dimensionless.



The WST identities require that, **at each perturbative order**, the gauge-boson self-energies

satisfy the equations

$$p_\mu p_\nu \Pi_{\mu\nu,AA}^{(n)} = 0$$

$$p_\mu p_\nu \Pi_{\mu\nu,AZ}^{(n)} + ip_\mu M_0 \Pi_{\mu,A\phi_0}^{(n)} = 0$$

$$p_\mu p_\nu \Pi_{\mu\nu,ZZ}^{(n)} + M_0^2 \Pi_{\phi_0\phi_0}^{(n)} + 2ip_\mu M_0 \Pi_{\mu,Z\phi_0}^{(n)} = 0$$

$$p_\mu p_\nu \Pi_{\mu\nu,WW}^{(n)} + M^2 \Pi_{\phi\phi}^{(n)} + 2ip_\mu M \Pi_{\mu,W\phi}^{(n)} = 0, \quad (34)$$



which imply the following relations among the form factors D , P , G , and R

$$D_{AA}^{(n)} + p^2 P_{AA}^{(n)} = 0 \quad (35)$$

$$D_{AZ}^{(n)} + p^2 P_{AZ}^{(n)} + M_0^2 G_{A\phi_0}^{(n)} = 0 \quad (36)$$

$$p^2 D_{ZZ}^{(n)} + p^4 P_{ZZ}^{(n)} + M_0^2 R_{\phi_0\phi_0}^{(n)} = -2 M_0^2 p^2 G_{Z\phi_0}^{(n)} \quad (37)$$

$$p^2 D_{WW}^{(n)} + p^4 P_{WW}^{(n)} + M^2 R_{\phi\phi}^{(n)} = -2 M^2 p^2 G_{W\phi}^{(n)}. \quad (38)$$

The subscripts A , Z , W , ϕ and ϕ_0 clearly indicate the SM fields. We have verified these WST Identities at the two-loop level (i.e. $n = 2$) with our code `GraphShot`.



WSTI at two loops: the role of reducible diagrams

At any given order in the coupling constant expansion, **the SM gauge boson self-energies satisfy the WSTI** (34). For $n \geq 2$, the quantities $\Pi_{ij}^{(n)}$ contain both one-particle irreducible (1PI) and reducible (1PR) contributions. At $\mathcal{O}(g^4)$, the SM $\Pi_{ij}^{(n)}$ functions contain the following *irreducible* topologies:

eight two-loop topologies,

three one-loop topologies with a β_t vertex,

four one-loop topologies with a Γ_1 vertex,

and **one** tree-level diagram with a two-leg $\mathcal{O}(g^4)$ β_t or Γ vertex .



Reducible $\mathcal{O}(g^4)$ graphs involve the product of two $\mathcal{O}(g^2)$ ones:

two one-loop diagrams,

one one-loop diagram and a tree-level diagram with a $\mathcal{O}(g^2)$ two-leg vertex insertion,

or two tree-level diagrams, each with a $\mathcal{O}(g^2)$ two-leg vertex insertion.

There are also $\mathcal{O}(g^4)$ topologies containing tadpoles but, as we discussed in previous sections, their contributions add up to zero as a consequence of our choice for β_t .

In the following we analyze the structure of the $\mathcal{O}(g^4)$ WSTI for photon, Z , and W self-energies, as well as for the photon– Z mixing, emphasizing the role played by the reducible diagrams.



The photon self-energy

The contribution of the **1PR diagrams** to the photon self-energy at $\mathcal{O}(g^4)$ is given, in the 't Hooft–Feynman gauge, by (with obvious notation)

$$\Pi_{\mu\nu,AA}^{(2)R} = \frac{1}{(2\pi)^4 i} \left[\frac{1}{p^2} \tilde{\Pi}_{\mu\nu,AA}^{(2)R} + \frac{1}{p^2 + M_0^2} \hat{\Pi}_{\mu\nu,AA}^{(2)R} \right], \quad (39)$$

where

$$\tilde{\Pi}_{\mu\nu,AA}^{(2)R} = \Pi_{\mu\alpha,AA}^{(1)} \Pi_{\alpha\nu,AA}^{(1)} \quad \hat{\Pi}_{\mu\nu,AA}^{(2)R} = \Pi_{\mu\alpha,AZ}^{(1)} \Pi_{\alpha\nu,ZA}^{(1)} + \Pi_{\mu,A\phi_0}^{(1)} \Pi_{\nu,\phi_0A}^{(1)}.$$



It is interesting to consider separately the reducible diagrams that involve an intermediate photon propagator ($\tilde{\Pi}_{\mu\nu,AA}^{(2)R}$) and those including an intermediate Z or ϕ_0 propagator ($\hat{\Pi}_{\mu\nu,AA}^{(2)R}$). By employing the definitions given in the previous subsection and eq. (35) with $n = 1$, one verifies that $\tilde{\Pi}_{\mu\nu,AA}^{2R}$ obeys the **photon WSTI** by itself,

Theorem

$$p_\mu p_\nu \tilde{\Pi}_{\mu\nu,AA}^{(2)R} = p^2 \left[D_{AA}^{(1)} + p^2 P_{AA}^{(1)} \right]^2 = 0. \quad (40)$$



This is not the case for $\hat{\Pi}_{\mu\nu,AA}^{(2)R}$, although most of its contributions cancel when contracted by $p_\mu p_\nu$ as a consequence of eq. (36) ($n = 1$),

$$p_\mu p_\nu \hat{\Pi}_{\mu\nu,AA}^{(2)R} = p^2 M_0^2 \left(p^2 + M_0^2 \right) \left[G_{A\phi_0}^{(1)} \right]^2. \quad (41)$$

The only diagrams contributing to the $A-\phi_0$ mixing up to $\mathcal{O}(g^2)$ are those with a $W-\phi$ or **FP ghosts** loop, and the tree-level diagram with a **Γ insertion**. Their contribution, in the 'tHooft–Feynman gauge, is

$$G_{A\phi_0}^{(1)} = (2\pi)^4 i sc \left[2B_0(p^2, M, M) + 16\pi^2 \Gamma_1 \right]. \quad (42)$$

A direct calculation (e.g. with **GraphShot**) shows that this residual contribution of the reducible diagrams to the $\mathcal{O}(g^4)$ photon WSTI, eq. (41), is exactly canceled by the contribution of the $\mathcal{O}(g^4)$ irreducible diagrams, which include **two-loop diagrams** as well as one-loop graphs with a **two-leg vertex insertion**.



Dyson resummed propagators and their WSTI

Dyson resummed propagators

We will now present the **Dyson resummed propagators** for the electroweak gauge bosons. We will then employ the results of sec. 1 to show explicitly, up to terms of $\mathcal{O}(g^4)$, that the resummed propagators **satisfy the WST identities**. Following definition (32) for Π_{ij} , the function Π'_{ij} represents the **sum of all 1PI diagrams** with two external boson fields, i and j , **to all orders** in perturbation theory (as usual, the external Born propagators are not to be included in the expression for Π'_{ij}).



As we did in eqs. (33), we write explicitly its ,

Lorentz structure

$$\Pi'_{\mu\nu, VV} = D'_{VV} \delta_{\mu\nu} + P'_{VV} p_\mu p_\nu \quad (43)$$

$$\Pi'_{\mu, VS} = -ip_\mu M_S G'_{VS} \quad \Pi'_{SS} = R'_{SS}, \quad (44)$$

where V and S indicate SM vector and scalar fields, and p_μ is the incoming momentum of the vector boson [note: $\Pi'_{\mu, SV} = -\Pi'_{\mu, VS}$].



We also introduce the

transverse and longitudinal projectors

$$t^{\mu\nu} = \delta_{\mu\nu} - \frac{p_\mu p_\nu}{p^2}, \quad l^{\mu\nu} = \frac{p_\mu p_\nu}{p^2},$$

$$t^{\mu\alpha} t^{\alpha\nu} = t^{\mu\nu}, \quad l^{\mu\alpha} l^{\alpha\nu} = l^{\mu\nu}, \quad t^{\mu\alpha} l^{\alpha\nu} = 0,$$

$$\Pi_{\mu\nu, VV}^l = D_{VV}^l t_{\mu\nu} + L_{VV}^l l_{\mu\nu}, \quad L_{VV}^l = D_{VV}^l + p^2 P_{VV}^l. \quad (45)$$



The full propagator for a **field i which mixes with a field j** via the function Π'_{ij} is given by the perturbative series

$$\begin{aligned}\bar{\Delta}_{ij} &= \Delta_{ij} + \Delta_{ij} \sum_{n=0}^{\infty} \prod_{l=1}^{n+1} \sum_{k_l} \Pi'_{k_{l-1}k_l} \Delta_{k_l k_l} \\ &= \Delta_{ij} + \Delta_{ij} \Pi'_{ij} \Delta_{ij} + \Delta_{ij} \sum_{k_1=i,j} \Pi'_{ik_1} \Delta_{k_1 k_1} \Pi'_{k_1 i} \Delta_{ij} + \dots,\end{aligned}\tag{46}$$

where $k_0 = k_{n+1} = i$, while for $l \neq n + 1$, k_l can be i or j . Δ_{ij} is the **Born propagator of the field i** .



We rewrite Eq.(46) as

$$\bar{\Delta}_{ii} = \Delta_{ii} [1 - (\Pi \Delta)_{ii}]^{-1}, \quad (47)$$

and refer to $\bar{\Delta}_{ii}$ as the *resummed propagator*. The quantity $(\Pi \Delta)_{ii}$ is the sum of all the possible products of Born propagators and self-energies, starting with a 1PI self-energy Π'_{ii} , or transition Π'_{ij} , and ending with a propagator Δ_{ij} , such that each element of the sum cannot be obtained as a product of other elements in the sum.



A diagrammatic representation of $(\Pi \Delta)_{ij}$ is the following,

$$(\Pi \Delta)_{ij} = \text{white blob} \text{---} \text{dotted line} + \text{gray blob} \text{---} \text{solid line} \text{---} \text{gray blob} \text{---} \text{dotted line} + \text{gray blob} \text{---} \text{solid line} \text{---} \text{black blob} \text{---} \text{solid line} \text{---} \text{gray blob} \text{---} \text{dotted line} + \dots$$

where the **Born propagator** of the field i (j) is represented by a **dotted (solid) line**, the **white blob** is the i **1PI self-energy**, and the **dots at the end** indicate a sum running over an infinite number of $1\text{PI } j$ **self-energies (black blobs)** inserted between two $1\text{PI } i$ - j **transitions (gray blobs)**.



It is also useful to define, as an auxiliary quantity, the *partially resummed propagator* for the field i , $\hat{\Delta}_{ii}$, in which we resum only the proper 1PI self-energy insertions Π'_{ii} , namely,

$$\hat{\Delta}_{ii} = \Delta_{ii} [1 - \Pi'_{ii} \Delta_{ii}]^{-1}. \quad (48)$$

If the particle i were not **mixing** with j through **loops or two-leg vertex insertions**, $\hat{\Delta}_{ii}$ would coincide with the resummed propagator $\bar{\Delta}_{ii}$.



$\hat{\Delta}_{ij}$ can be graphically depicted as

$$\hat{\Delta}_{ij} = \text{---}\blacktriangleright\text{---} + \text{---}\blacktriangleright\bigcirc\text{---}\blacktriangleright\text{---} + \text{---}\blacktriangleright\bigcirc\text{---}\blacktriangleright\bigcirc\text{---}\blacktriangleright\text{---} + \dots$$



Partially resummed propagators allow for a compact expression for $(\Pi \Delta)_{ii}$,

$$(\Pi \Delta)_{ii} = \Pi'_{ii} \Delta_{ii} + \Pi'_{ij} \hat{\Delta}_{jj} \Pi'_{ji} \Delta_{ii}, \quad (49)$$

so that the resummed propagator of the field i can be cast in the form

$$\bar{\Delta}_{ii} = \Delta_{ii} \left[1 - \left(\Pi'_{ii} + \Pi'_{ij} \hat{\Delta}_{jj} \Pi'_{ji} \right) \Delta_{ii} \right]^{-1}. \quad (50)$$

We can also define a resummed propagator for the i - j transition. In this case there is no corresponding Born propagator, and the resummed one is given by the sum of all possible products of 1PI i and j self-energies, transitions, and Born propagators starting with Δ_{ii} and ending with Δ_{jj} . This sum can be simply expressed in the following compact form,

$$\bar{\Delta}_{ij} = \bar{\Delta}_{ii} \Pi'_{ij} \hat{\Delta}_{jj}. \quad (51)$$



Dressed propagators

Suppose that we have a **simple model** with an interaction Lagrangian

$$L = \frac{g}{2} \Phi(x) \phi^2(x). \quad (52)$$

The mass M of the Φ -field and m of the ϕ -field be such that the Φ -field be **unstable**. Let Δ_i be the **lowest order propagators** and $\overline{\Delta}_i$ the **one-loop dressed propagators**, i.e.

$$\overline{\Delta}_\Phi = \frac{\Delta_\Phi}{1 - \Delta_\Phi \Sigma_{\Phi\Phi}}, \quad \overline{\Delta}_\phi = \frac{\Delta_\phi}{1 - \Delta_\phi \Sigma_{\phi\phi}}, \quad (53)$$

etc. In **fixed order perturbation theory**, the ϕ **self-energy** is given in **Fig. 1**.



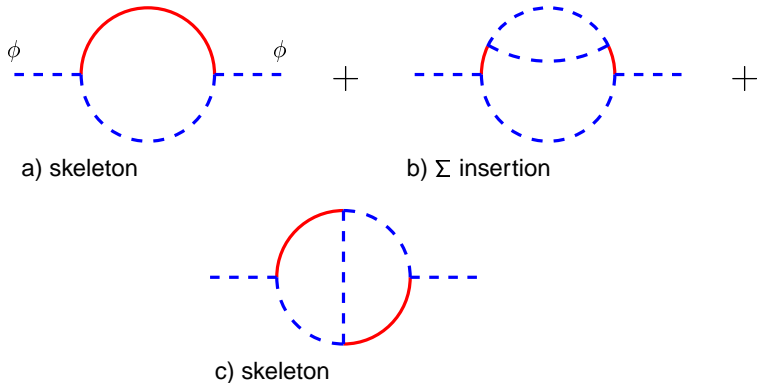


Figure: The ϕ self-energy with skeleton expansion, diagrams a) and c), and insertion of a sub-loop $\Sigma_{\phi\phi}$, diagram b).



ϕ imaginary part

Note that the **imaginary part** of $\Sigma_{\phi\phi}$ is **non-zero** only for

$$\begin{aligned} -p^2 > 9 m^2, & \quad (\text{the three-particle cut of diagram b) in Fig. 1), \\ & \quad \text{if } m \ll M. \end{aligned} \tag{54}$$



When we use **dressed propagators** only **diagrams a) and c)** are retained in **Fig. 1** (for two-loop accuracy) but in **a)** we use $\overline{\Delta}_\phi$ with **one-loop accuracy**:

$$\Sigma_{\phi\phi}^{(a)} = \int \frac{d^n q_2}{\left(q_2^2 + M^2 - \frac{g^2}{16\pi^2} \Sigma_{\phi\phi}(q_2^2)\right) \left((q_2 + p)^2 + m^2\right)},$$

$$\Sigma_{\phi\phi}(q_2^2) = B_0(q_2^2; m, m), \quad (55)$$

where we assume $p^2 < 0$.



Since the **complex Φ pole** is defined by

$$M^2 - s_M - \frac{g^2}{16\pi^2} \Sigma_{\Phi\Phi}(-s_M) = 0, \quad (56)$$

we write the **inverse (dressed) propagator** as

$$\left[1 - \frac{g^2}{16\pi^2} \frac{\Sigma_{\Phi\Phi}(q_2^2) - \Sigma_{\Phi\Phi}(-s_M)}{q_2^2 + s_M} \right] (q_2^2 + s_M), \quad (57)$$

expand in g as if we were in a gauge theory with problems of gauge parameter dependence and obtain

$$\begin{aligned} \Sigma_{\phi\phi}^{(a)} &= g^2 \int \frac{d^n q}{(q^2 + s_M) ((q+p)^2 + m^2)} \\ &\times \left[1 + \frac{g^2}{16\pi^2} \frac{\Sigma_{\Phi\Phi}(q^2) - \Sigma_{\Phi\Phi}(-s_M)}{q^2 + s_M} \right] \end{aligned} \quad (58)$$



$$\begin{aligned}
&= \frac{i}{2} g^2 \pi^2 B_0 \left(1, 1; p^2; s_M, m^2 \right) + i \frac{g^4}{16} S^E \left(p^2; m^2, m^2, s_M, m^2, s_M \right) \\
&+ i \frac{g^4}{16} B_0 \left(2, 1; p^2; s_M, m^2 \right) \left[\Delta_{UV} - \ln \frac{m^2}{\mu^2} + 2 - \beta \ln \frac{\beta + 1}{\beta - 1} \right], \quad (59)
\end{aligned}$$

where

$$\beta^2 = 1 - 4 \frac{m^2}{s_M}. \quad (60)$$



More on dressed propagators

Note that there is an **interplay** between using **dressed propagators** for all **internal lines of a diagram** and **combinatorial factors** and **number of diagrams** with and without **dressed propagators**.

Note that the poles in the q^0 **complex plane** remain in the same quadrants as in the **Feynman prescription** and **Wick rotation** can be carried out, as usual. Evaluation of diagrams with **complex masses** does not pose a **serious problem**; in the **analytical approach** one should, however, pay the due attention to **splitting of logarithms**.



Consider a B_0 function,

$$B_0(p^2; M_1, M_2) = \Delta_{UV} - \int_0^1 dx \frac{\chi(x)}{\mu^2},$$
$$\chi(x) = -p^2 x^2 + (p^2 + M_2^2 - M_1^2)x + M_1^2, \quad (61)$$

where one usually writes

$$\ln \frac{\chi(x)}{\mu^2} = \ln\left(-\frac{p^2}{\mu^2} - i\delta\right) + \ln(x - x_-) + \ln(x - x_+). \quad (62)$$

Since $\text{Im} \chi(x)$ does not change sign with in $[0, 1]$ the correct recipe for $M^2 = m^2 - i m \gamma$ is

$$\ln \frac{\chi(x)}{\mu^2} = \ln |p^2| + \ln(x - x_-) + \theta(-p^2) \left[\ln(x - x_+) + \eta(-x_-, -x_+) \right]$$
$$+ \theta(p^2) \left[\ln(x_+ - x) + \eta(-x_-, x_+) \right]. \quad (63)$$



In the **numerical treatment**, instead, **no splitting** is performed and no special care is needed.

A **t -channel propagator** deserves some additional comment: one should not confuse the **position of the pole** which is always at $\mu^2 - i\mu\gamma$ with the fact that a **dressed propagator function** is **real in the t -channel**.



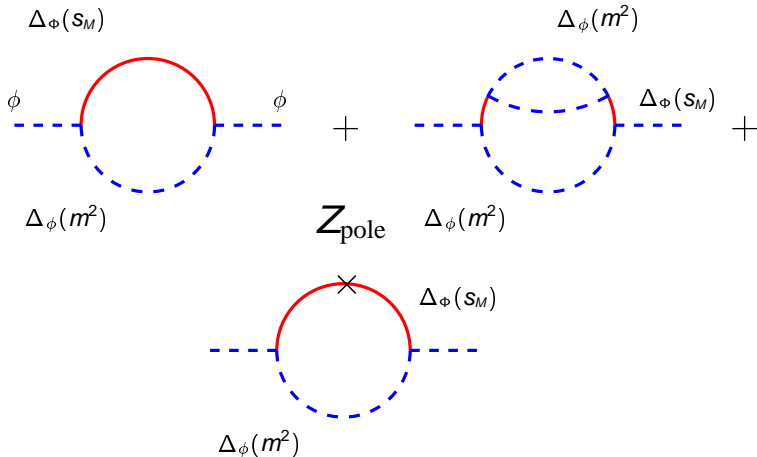


Figure: Diagram b) of Fig. 1 with one-loop dressed Φ propagators is equivalent, up to $\mathcal{O}(g^4)$, to the sum of three diagrams with lowest order propagators μ with the Φ mass replaced with the Φ complex pole. The Z_{pole} vertex is given in Eq.(64)



Theorem

Therefore, using *one-loop* diagrams with *one-loop dressed* Φ propagators is equivalent, to $\mathcal{O}(g^4)$, to use the sum of the three diagrams of Fig. 2 where Φ propagators are at *lowest order* but with *complex mass* s_M and where the vertex Z_{pole} is defined by

$$Z_{\text{pole}} = \frac{g^2}{16\pi^2} B_0(-s_M; m, m). \quad (64)$$



The charged sector

We now apply Eq.(48), Eq.(50), Eq.(51)) to W and charged Goldstone boson fields. The *partially resummed propagator* of the *charged Goldstone scalar* follows immediately from Eq.(48). The Born W and ϕ propagators in the 't Hooft–Feynman gauge are

$$\Delta_{WW}^{\mu\nu} = \frac{\delta_{\mu\nu}}{p^2 + M^2}, \quad \Delta_{\phi\phi} = \frac{1}{p^2 + M^2}, \quad (65)$$

where, for simplicity of notation, we have dropped the coefficients $(2\pi)^4 i$.



In the same gauge, the partially resummed ϕ and W propagators are

$$\hat{\Delta}_{\phi\phi} = \Delta_{\phi\phi} [1 - \Pi'_{\phi\phi} \Delta_{\phi\phi}]^{-1} = [\rho^2 + M^2 - R'_{\phi\phi}]^{-1} \quad (66)$$

$$\hat{\Delta}_{WW}^{\mu\nu} = \frac{1}{\rho^2 + M^2 - D'_{WW}} \left(\delta_{\mu\nu} + \frac{\rho_\mu \rho_\nu P'_{WW}}{\rho^2 + M^2 - D'_{WW} - \rho^2 P'_{WW}} \right). \quad (67)$$



Equation (67) assumes a more compact form when expressed in terms of the transverse and longitudinal projectors $t_{\mu\nu}$ and $l_{\mu\nu}$,

$$\hat{\Delta}_{WW}^{\mu\nu} = \frac{t^{\mu\nu}}{p^2 + M^2 - D'_{WW}} + \frac{l^{\mu\nu}}{p^2 + M^2 - L'_{WW}}. \quad (68)$$

The resummed W and ϕ propagators can be then derived from Eq.(50),

$$\bar{\Delta}_{\phi\phi} = \left[p^2 + M^2 - R'_{\phi\phi} - \frac{p^2 M^2 (G'_{W\phi})^2}{p^2 + M^2 - L'_{WW}} \right]^{-1} \quad (69)$$

$$\bar{\Delta}_{WW}^{\mu\nu} = \frac{t^{\mu\nu}}{p^2 + M^2 - D'_{WW}} + l^{\mu\nu} \left[p^2 + M^2 - L'_{WW} - \frac{p^2 M^2 (G'_{W\phi})^2}{p^2 + M^2 - R'_{\phi\phi}} \right]^{-1}. \quad (70)$$



The **resummed propagator** for the **W - ϕ transition** is provided by Eq.(51),

$$\bar{\Delta}_{W\phi}^{\mu} = \frac{-ip_{\mu}MG'_{\phi W}}{p^2 + M^2 - R'_{\phi\phi}} \left[p^2 + M^2 - L'_{WW} - \frac{p^2 M^2 (G'_{W\phi})^2}{p^2 + M^2 - R'_{\phi\phi}} \right]^{-1}. \quad (71)$$

We will now show explicitly, up to terms of $\mathcal{O}(g^4)$, that the **resummed propagators** defined above satisfy the **following WST identity**:

Theorem

$$p_{\mu} p_{\nu} \bar{\Delta}_{WW}^{\mu\nu} + ip_{\mu} M \bar{\Delta}_{W\phi}^{\mu} - ip_{\nu} M \bar{\Delta}_{\phi W}^{\nu} + M^2 \bar{\Delta}_{\phi\phi} = 1, \quad (72)$$



which, in turn, is satisfied if

$$p^2 M^2 (G'_{W\phi})^2 + M^2 R'_{\phi\phi} + p^2 L'_{WW} - R'_{\phi\phi} L'_{WW} + 2p^2 M^2 G'_{W\phi} = 0. \quad (73)$$

This equation can be verified explicitly, up to terms of $\mathcal{O}(g^4)$, using the WSTI for the **W self-energy**: at $\mathcal{O}(g^2)$ Eq.(73) becomes simply

$$M^2 R_{\phi\phi}^{(1)} + p^2 L_{WW}^{(1)} + 2p^2 M^2 G_{W\phi}^{(1)} = 0, \quad (74)$$

which coincides with eq. (38) for $n = 1$.



To prove Eq.(73) at $\mathcal{O}(g^4)$ we use (for simplicity of notation, in this section we dropped the coefficients $(2\pi)^4 i$.)

$$p^2 M^2 \left(G_{W\phi}^{(1)} \right)^2 + M^2 R_{\phi\phi}^{(2)'} + p^2 L_{WW}^{(2)'} - R_{\phi\phi}^{(1)} L_{WW}^{(1)} + 2p^2 M^2 G_{W\phi}^{(2)'} = 0. \quad (75)$$



The LQ basis

For the purpose of the renormalization, it is more convenient to extract from the quantities defined in the previous sections the factors involving the weak mixing angle θ . To achieve this goal, we employ the LQ basis, which relates the photon and Z fields to a new pair of fields, L and Q :

$$\begin{pmatrix} Z_\mu \\ A_\mu \end{pmatrix} = \begin{pmatrix} c & 0 \\ s & 1/s \end{pmatrix} \begin{pmatrix} L_\mu \\ Q_\mu \end{pmatrix}. \quad (76)$$



Consider the fermion currents j_A^μ and j_Z^μ coupling to the photon and to the Z . As the Lagrangian must be left unchanged under this transformation, namely $j_Z^\mu Z_\mu + j_A^\mu A_\mu = j_L^\mu L_\mu + j_Q^\mu Q_\mu$, the currents transform as

$$\begin{pmatrix} j_Z^\mu \\ j_A^\mu \end{pmatrix} = \begin{pmatrix} 1/c & -s^2/c \\ 0 & s \end{pmatrix} \begin{pmatrix} j_L^\mu \\ j_Q^\mu \end{pmatrix}. \quad (77)$$



If we rewrite the SM Lagrangian in terms of the fields L and Q , and perform the same transformation (76) on the FP ghosts fields [from (X_A, X_Z) to (X_L, X_Q)], then all the interaction terms of the SM Lagrangian are independent of θ . Note that this is true only if the relation $M/c = M_0$ is employed, wherever necessary, to remove the remaining dependence on θ . In this way the dependence on the weak mixing angle is moved to the kinetic terms of the L and Q fields which, clearly, are not mass eigenstates.

The relevant fact for our discussion is that the couplings of Z , photon, X_Z and X_A are related to those of the fields L and Q , X_L and X_Q by identities like the one described, in a diagrammatic way, in the following figure:



$$\begin{array}{ccc}
 \begin{array}{c} Z \\ \text{---} \\ \text{---} \swarrow \nearrow \\ f \quad \bar{f} \end{array} & = \frac{1}{c} & \begin{array}{c} L \\ \text{---} \\ \text{---} \swarrow \nearrow \\ f \quad \bar{f} \end{array} \\
 \begin{array}{c} A \\ \text{---} \\ \text{---} \swarrow \nearrow \\ W \quad Z \end{array} & = \frac{s}{c} & \begin{array}{c} Q \\ \text{---} \\ \text{---} \swarrow \nearrow \\ W \quad L \end{array} \\
 & & \begin{array}{c} Q \\ \text{---} \\ \text{---} \swarrow \nearrow \\ f \quad \bar{f} \end{array} \\
 & & \begin{array}{c} Q \\ \text{---} \\ \text{---} \swarrow \nearrow \\ W \quad Q \end{array} \\
 & & = -\frac{s^2}{c} \\
 & & = -\frac{s^3}{c}
 \end{array}$$



As the couplings of the fields L , Q , X_L and X_Q do not depend on θ , all the dependence on this parameter is factored out in the coefficients in the r.h.s. of these identities.

Since θ appears only in the couplings of the fields A , Z , X_A and X_Z (once again, the relation $M/c = M_0$ must also be employed, wherever necessary), it is possible to single out this parameter in the two-loop self-energies of the vector bosons. Consider, for example, the transverse part of the photon two-loop self-energy $D_{AA}^{(2)}$ (which includes the contribution of both *irreducible* and *reducible* diagrams). All diagrams contributing to $D_{AA}^{(2)}$ can be classified in two classes: those including (i) one internal A , Z , X_A or X_Z field, and (ii) those not containing any of these fields. The complete dependence on θ can be factored out by expressing the external photon couplings and the internal A , Z , X_A or X_Z couplings of the diagrams of class (i) in terms of the couplings of the fields L , Q , X_L and X_Q , namely



$$D_{AA}^{(2)} = s^2 \left[\frac{1}{c^2} f_1^{AA} + f_2^{AA} + s^2 f_3^{AA} \right], \quad (78)$$

where the functions f_i^{AA} ($i = 1, 2, 3$) are θ -independent. Similarly, we can factor out the θ dependence of the transverse part of the two-loop photon-Z mixing and Z self-energy,

$$D_{AZ}^{(2)} = \frac{s}{c} \left[\frac{1}{c^2} f_1^{AZ} + f_2^{AZ} + s^2 f_3^{AZ} + s^4 f_4^{AZ} \right], \quad (79)$$

$$D_{ZZ}^{(2)} = \frac{1}{c^2} \left[\frac{1}{c^2} f_1^{ZZ} + f_2^{ZZ} + s^2 f_3^{ZZ} + s^4 f_4^{ZZ} + s^6 f_5^{ZZ} \right], \quad (80)$$



where, once again, the functions f_i^{AZ} and f_i^{ZZ} ($i = 1, \dots, 5$) do not depend on θ . Analogous relations hold for the longitudinal components of the two-loop self-energies.

We note that $D_{AZ}^{(2)}$ and $D_{ZZ}^{(2)}$ also contain a third class of diagrams containing more than one internal Z (or X_Z) field (up to three, in $D_{ZZ}^{(2)}$). However, the diagrams of this class involve the trilinear vertex ZHZ (or $\overline{X}_Z H X_Z$), which does not induce any new θ dependence.



However, from the point of view of renormalization it is more convenient to distinguish between the θ dependence originating from external legs and the one introduced by external legs. We define, to all orders,

$$D_{AA} = s^2 \Pi_{QQ; \text{ext}} p^2 = s^2 \sum_{n=1}^{\infty} \left(\frac{g^2}{16\pi^2} \right)^n \Pi_{QQ; \text{ext}}^{(n)} p^2,$$

$$D_{AZ} = \frac{s}{c} \Sigma_{AZ; \text{ext}} = \frac{s}{c} \sum_{n=1}^{\infty} \left(\frac{g^2}{16\pi^2} \right)^n \Sigma_{AZ; \text{ext}}^{(n)},$$

$$D_{ZZ} = \frac{1}{c^2} \Sigma_{ZZ; \text{ext}} = \frac{1}{c^2} \sum_{n=1}^{\infty} \left(\frac{g^2}{16\pi^2} \right)^n \Sigma_{ZZ; \text{ext}}^{(n)},$$

$$\Sigma_{AZ; \text{ext}}^{(n)} = \Sigma_{3Q; \text{ext}}^{(n)} - s^2 \Pi_{QQ; \text{ext}}^{(n)} p^2,$$

$$\Sigma_{ZZ; \text{ext}}^{(n)} = \Sigma_{33; \text{ext}}^{(n)} - 2s^2 \Sigma_{3Q; \text{ext}}^{(n)} + s^4 \Pi_{QQ; \text{ext}}^{(n)} p^2. \quad (81)$$



Furthermore, our procedure is such that

$$\Sigma_{3Q; \text{ext}}^{(n)} = \Pi_{3Q; \text{ext}}^{(n)} p^2, \quad (82)$$

with $\Pi_{3Q; \text{ext}}^{(n)}$ regular at $p^2 = 0$. At $\mathcal{O}(g^2)$ the *external* quantities are θ -independent while, at $\mathcal{O}(g^4)$ the relation with the coefficients of Eqs.(78)–(80) is

$$\begin{aligned} \Pi_{QQ; \text{ext}}^{(2)} p^2 &= \frac{1}{c^2} f_1^{AA} + f_2^{AA} + f_3^{AA} s^2, \\ \Sigma_{3Q; \text{ext}}^{(2)} &= \frac{1}{c^2} (f_1^{AA} + f_1^{AZ}) - f_1^{AA} + f_2^{AZ} + s^2 (f_2^{AA} + f_3^{AZ}) + s^4 (f_3^{AA} + f_4^{AZ}) \\ \Sigma_{33; \text{ext}}^{(2)} &= \frac{1}{c^2} (f_1^{AA} + 2 f_1^{AZ} + f_1^{ZZ}) - f_1^{AA} - 2 f_1^{AZ} + f_2^{ZZ} \\ &\quad + s^2 (-f_1^{AA} + 2 f_2^{AZ} + f_3^{ZZ}) + s^4 (f_2^{AA} + 2 f_3^{AZ} + f_4^{ZZ}) \\ &\quad + s^6 (f_3^{AA} + 2 f_4^{AZ} + f_5^{ZZ}), \end{aligned} \quad (83)$$

and s, c in Eq.(83) should be evaluated at $\mathcal{O}(g^0)$.



Consider the process $\bar{f}f \rightarrow \bar{h}h$; taking into account Dyson re-summed propagators and neglecting, for the moment, vertices and boxes we write

$$\begin{aligned}
 \mathcal{M}(\bar{f}f \rightarrow \bar{h}h) = (2\pi)^4 i \left[-e^2 Q_f Q_h \gamma^\mu \otimes \gamma^\mu \bar{\Delta}_{AA}^T \right. \\
 - \frac{eg}{2c} Q_f \gamma^\mu \otimes \gamma^\mu (\mathbf{v}_h + \mathbf{a}_h \gamma_5) \bar{\Delta}_{ZA}^T \\
 - \frac{eg}{2c} Q_h \gamma^\mu (\mathbf{v}_f + \mathbf{a}_f \gamma_5) \otimes \gamma^\mu \bar{\Delta}_{ZA}^T \\
 \left. - \frac{g^2}{4c^2} \gamma^\mu (\mathbf{v}_f + \mathbf{a}_f \gamma_5) \otimes \gamma^\mu (\mathbf{v}_h + \mathbf{a}_h \gamma_5) \bar{\Delta}_{ZZ}^T \right] \quad (84)
 \end{aligned}$$

where f and h are fermions with quantum numbers $Q_i, I_{3i}, i = f, h$;



furthermore we have introduced

$$v_f = l_{3f} - 2 Q_f s^2, \quad a_f = l_{3f}, \quad (85)$$

with $e^2 = g^2 s^2$. Always neglecting terms proportional to fermion masses it is useful to introduce an effective weak-mixing angle as follows:

Definition

$$s_{\text{eff}}^2 = s^2 \left[1 - \frac{\Pi_{AZ; \text{ext}}}{1 - s^2 \Pi_{AA; \text{ext}}} \right], \quad V_f = l_{3f} - 2 Q_f s_{\text{eff}}^2. \quad (86)$$



The amplitude of Eq.(84) can be cast into the following form:

$$\begin{aligned} \mathcal{M}(\bar{f}f \rightarrow \bar{h}h) = (2\pi)^4 i \left[-\gamma^\mu \otimes \gamma^\mu \frac{1}{1 - s^2 \Pi_{AA; \text{ext}}} \frac{e^2 Q_f Q_h}{p^2} \right. \\ \left. - \frac{g^2}{4c^2} \gamma^\mu (V_f + \mathbf{a}_f \gamma_5) \otimes \gamma^\mu (V_h + \mathbf{a}_h \gamma_5) \bar{\Delta}_{ZZ}^T \right]. \quad (87) \end{aligned}$$

The functions $\Pi_{AA; \text{ext}}$, $\Pi_{AZ; \text{ext}}$ and $\Sigma_{ZZ; \text{ext}}$ start at $\mathcal{O}(g^2)$ in perturbation theory. Eq.(87) shows the nice **effect of absorbing – to all orders – non-diagonal transitions into a redefinition of s^2** and forms the basis for introducing **renormalization equations in the neutral sector**, e.g. the one associated with the fine-structure constant α . Questions related to gauge-parameter independence of Dyson re-summation, e.g. in Eq.(86), will not be addressed here.



Part II

Lecture II



The QED case

To understand renormalization at the two-loop level we consider first the case of **pure QED** where we have

$$\Pi_{\text{QED}}(s, m) = \frac{e^2}{16\pi^2} \Pi^{(1)}(s, m) + \frac{e^4}{256\pi^4} \Pi^{(2)}(s, m), \quad (88)$$

where $p^2 = -s$ and where we have indicated a dependence of the result on the **(bare) electron mass**. Suppose that we compute the **two-loop contribution** (3 diagrams) in the **limit $m = 0$** . The result is

$$\Pi^{(2)}(s, 0) = -\frac{4}{\epsilon} + \mathcal{O}(1), \quad (89)$$

where $n = 4 - \epsilon$. This is a **well-known** result which shows the **cancellation of the double ultraviolet pole** as well as of **any non-local residue**. The latter is related to the fact that the four one-loop diagrams with one-loop counterterms cancel due to a **Ward identity**. Let us repeat the calculation with a **non-zero electron mass**;



The QED case

To understand renormalization at the two-loop level we consider first the case of **pure QED** where we have

$$\Pi_{\text{QED}}(s, m) = \frac{e^2}{16\pi^2} \Pi^{(1)}(s, m) + \frac{e^4}{256\pi^4} \Pi^{(2)}(s, m), \quad (88)$$

where $p^2 = -s$ and where we have indicated a dependence of the result on the **(bare) electron mass**. Suppose that we compute the **two-loop contribution** (3 diagrams) in the **limit $m = 0$** . The result is

$$\Pi^{(2)}(s, 0) = -\frac{4}{\epsilon} + \mathcal{O}(1), \quad (89)$$

where $n = 4 - \epsilon$. This is a **well-known** result which shows the **cancellation of the double ultraviolet pole** as well as of **any non-local residue**. The latter is related to the fact that the four one-loop diagrams with one-loop counterterms cancel due to a **Ward identity**. Let us repeat the calculation with a **non-zero electron mass**;



after *scalarization* of the result we consider the **ultraviolet divergent parts** of the various diagrams. Collecting all the terms we obtain

$$\Pi^{(2)}(s, m) = -\frac{1}{\epsilon} \left[4 \left(1 + 24 \frac{m^2}{s} \right) + 192 \frac{m^4}{s^2} \frac{1}{\beta(m)} \ln \frac{\beta(m) + 1}{\beta(m) - 1} \right] + \mathcal{O}(1). \quad (90)$$

Note that the ***m* dependent** part is not only **finite** but also **zero** in the **limit** $s \rightarrow 0$; indeed, in the limit $s \rightarrow 0$ and with $\mu^2 = m^2/s - i\delta$ we have

$$\beta = 2i\mu - \frac{i}{2\mu} + \mathcal{O}(\mu^{-2}), \quad \frac{1}{\beta} \ln \frac{\beta + 1}{\beta - 1} = -\frac{1}{2\mu^2}, \quad (91)$$

so that

$$\Pi^{(2)}(0, m) = -\frac{4}{\epsilon} + \Pi_{\text{fin}}^{(2)}(0, m). \quad (92)$$



Eq.(92) is the **main ingredient** to build our **renormalization equation** and contains only **bare parameters**, in the true spirit of the **fitting equations** that express a measurable input, α in this case, as a function of **bare parameters**, **e and m** in this case, and of **ultraviolet singularities**.

To make a prediction, **the running of α in this case**, is a different issue: the **scattering of two charged particles** is proportional to

$$\frac{e^2}{1 - f(s)} = e^2 \left[1 + f(s) + f^2(s) + \dots \right],$$
$$f(s) = \frac{e^2}{16\pi^2} \Pi^{(1)}(s) + \frac{e^4}{(16\pi^2)^2} \Pi^{(2)}(s) + \mathcal{O}(e^6). \quad (93)$$



Renormalization

Renormalization amounts to substituting

$$e^2 = 4\pi\alpha - \alpha^2 \Pi^{(1)}(0) + \frac{\alpha^3}{4\pi} \left\{ \left[\Pi^{(1)}(0) \right]^2 - \Pi^{(2)}(0) \right\} + \mathcal{O}(\alpha^4), \quad (94)$$

with the following result

$$\begin{aligned} \frac{e^2}{1-f(s)} &= 4\pi\alpha \left\{ 1 + \frac{\alpha}{4\pi} \Pi_R^{(1)}(s) + \left(\frac{\alpha}{4\pi} \right)^2 \left[\Pi_R^{(1)}(s) \Pi_R^{(1)}(s) \right. \right. \\ &\quad \left. \left. + \Pi_R^{(2)}(s) \right] + \mathcal{O}(\alpha^3) \right\}, \\ \Pi_R^{(n)}(s) &= \Pi^{(n)}(s) - \Pi^{(n)}(0). \end{aligned} \quad (95)$$



If our result has to be **ultraviolet finite** then the poles in $\Pi^{(n)}(s)$ should not depend on the **scale s** . This is obviously true for the one-loop result but **what is the origin of the scale-dependent extra term in Eq.(90)?** One should take into account that

$$\begin{aligned} \Pi^{(1)}(s, m) = & -\frac{8}{3} \frac{1}{\epsilon} + \frac{4}{3} \left[\ln \frac{m^2}{M^2} + \left(1 + 2 \frac{m^2}{s} \beta(m)\right) \ln \frac{\beta(m) + 1}{\beta(m) - 1} \right] \\ & - \frac{20}{9} + \frac{4}{3} \Delta_{UV} - \frac{16}{3} \frac{m^2}{s}, \end{aligned} \quad (96)$$

and that m is the **bare electron mass**. To proceed step-by-step we introduce a **renormalized electron mass** which is given by

$$m = m_R \left[1 + \frac{e^2}{16\pi^2} \left(-\frac{6}{\epsilon} + \text{finite part} \right) \right]. \quad (97)$$



showing cancellation of the ultraviolet poles in $\Pi_R^{(n)}(s, m_R)$ with $n = 1, 2$. Of course Eq.(97) is not yet a true renormalization equation since the latter should contain the **physical electron mass m_e** and not the **intermediate parameter m_R** but the relation between the two is **ultraviolet finite**. All of this is telling us that a **renormalization equation** has the structure

$$\rho_{\text{phys}} = f\left(\frac{1}{\epsilon}, \rho_{\text{bare}}\right), \quad (100)$$

where the **residue of the ultraviolet poles must be local**. A prediction,

$$O\left(\frac{1}{\epsilon}, \rho_{\text{bare}}\right) \equiv O(\rho_{\text{phys}}), \quad (101)$$

gives a **finite quantity** that can be computed in terms of **some input parameter set**.



The SM case

In the **full standard model** the one-loop result is

$$\Pi^{(1)} = \Pi_{\text{bos}}^{(1)} + \sum_l \Pi_l^{(1)} + \Pi_{tb}^{(1)} + \Pi_{udcs}^{(1)}. \quad (102)$$

We introduce

$$x_W = \frac{M_W^2}{s}, \quad x_l = \frac{m_l^2}{M_W^2}, \quad \text{etc,}$$
$$\Delta_{UV} = \gamma + \ln \pi + \ln \frac{M_W^2}{\mu^2}, \quad L_\beta(x) = \ln \frac{\beta(x) + 1}{\beta(x) - 1}, \quad (103)$$



In the limit $\mathbf{s} \rightarrow \mathbf{0}$ we have

$$\begin{aligned}\Pi_{\text{bos}}^{(1)}(0) &= -3 \left(-\frac{2}{\epsilon} + \Delta_{UV} \right), \\ \Pi_l^{(1)}(0) &= \frac{4}{3} \left(-\frac{2}{\epsilon} + \Delta_{UV} \right) + \frac{4}{9} + \frac{4}{3} \ln x_l, \\ \Pi_{tb}^{(1)}(0) &= \frac{20}{9} \left(-\frac{2}{\epsilon} + \Delta_{UV} \right) + \frac{20}{27} + \frac{16}{9} \ln x_t + \frac{4}{9} \ln x_b.\end{aligned}\quad (104)$$

First we consider **fermion mass renormalization**, obtaining

$$m_f^2 = m_{fR}^2 \left(1 + 2 \frac{g^2}{16\pi^2} \frac{\delta Z_m^f}{\epsilon} \right), \quad (105)$$

with **renormalization constants** given by



fermion mass renormalization

lepton

$$\begin{aligned}\delta Z_m^l = & -\frac{3}{2} \frac{1}{c^4} x_H^{-1} - 3 \frac{1}{c^2} + 3 + \frac{3}{4} x_L \\ & + 2 \frac{x_L^2}{x_H} + 6 \frac{x_B^2}{x_H} + 6 \frac{x_T^2}{x_H} - \frac{3}{4} x_H - 3 x_H^{-1},\end{aligned}\quad (106)$$



b quark

$$\begin{aligned}\delta Z_m^b = & -\frac{3}{2} \frac{1}{c^4} x_H^{-1} + \frac{1}{3} \frac{1}{c^2} - \frac{1}{3} + \frac{3}{4} x_B - \frac{3}{4} x_T \\ & + 2 \frac{x_L^2}{x_H} + 6 \frac{x_B^2}{x_H} + 6 \frac{x_T^2}{x_H} - \frac{3}{4} x_H - 3 x_H^{-1},\end{aligned}\quad (107)$$



t quark

$$\begin{aligned}\delta Z_m^t = & -\frac{3}{2} \frac{1}{c^4} x_H^{-1} - \frac{2}{3} \frac{1}{c^2} + \frac{2}{3} - \frac{3}{4} x_B + \frac{3}{4} x_T \\ & + 2 \frac{x_L^2}{x_H} + 6 \frac{x_B^2}{x_H} + 6 \frac{x_T^2}{x_H} - \frac{3}{4} x_H - 3 x_H^{-1}.\end{aligned}\tag{108}$$



Consider the **fermionic part** of $\Pi^{(1)}$ relative to one fermion generation (ν_l, l, t and b) and perform **fermion mass renormalization**; we obtain

$$\Pi_{\text{fer}}^{(1)} \rightarrow \Pi_{\text{ferm}}^{(1)} + \frac{g^2}{\pi^2 \epsilon} \Delta \Pi_{\text{ferm}}^{(1)}, \quad (109)$$

where

$$\begin{aligned} \Pi_{\text{fer}}^{(1)} = & \frac{32}{9} \left(-\frac{2}{\epsilon} + \Delta_{UV} \right) + \frac{4}{3} \left(\ln x_L + \frac{1}{3} \ln x_B + \frac{4}{3} \ln x_T \right) \\ & - \frac{160}{27} - \frac{16}{3} x_W \left(x_L + \frac{1}{3} x_B + \frac{4}{3} x_T \right) + \frac{4}{3} (1 - 2 x_W x_L - 8 x_W^2 x_L^2) \\ & + \frac{4}{3} \beta^{-1} (x_W x_L) L_\beta(x_W x_L) + \frac{4}{9} \beta^{-1} (x_W x_B) L_\beta(x_W x_B) \\ & + \frac{16}{9} \beta^{-1} (x_W x_T) L_\beta(x_W x_T), \end{aligned} \quad (110)$$



$$\begin{aligned}
\Delta \Pi_{\text{ferm}}^{(1)} = & \frac{3}{2} c^{-4} x_W x_L x_H^{-1} + \frac{1}{2} c^{-4} x_W x_B x_H^{-1} + 2c^{-4} x_W x_T x_H^{-1} + 3c^{-2} x_W x_L \\
& - \frac{1}{9} c^{-2} x_W x_B + \frac{8}{9} c^{-2} x_W x_T - 6x_W x_L x_B^2 x_H^{-1} - 6x_W x_L x_T^2 x_H^{-1} + \dots \\
& + 2x_W^2 x_T^2 x_H - \frac{16}{9} x_W^2 x_T^2 - 2x_W^2 x_T^3 - 16x_W^2 x_T^4 x_H^{-1} \Big). \quad (111)
\end{aligned}$$



When we add the **two-loop** result we obtain

$$\frac{g^2}{16\pi^2} \Pi_{\text{fer}}^{(1)} + \frac{g^4}{(16\pi^2)^2} \Pi^{(2)} = \text{one loop} + \frac{g^4}{\pi^4} \left[R^{(2)} \epsilon^{-2} + R^{(1)} \epsilon^{-1} + \Pi_{\text{fin}} \right]. \quad (112)$$

The **two residues** are given by

$$\begin{aligned} R^{(2)} &= -\frac{11}{256}, \\ R^{(1)} &= \frac{11}{256} \Delta_{UV} + \frac{407}{27648} + \frac{9}{64} c^{-4} x_W x_H^{-1} - \frac{9}{128} c^{-2} x_W - \frac{131}{6912} c^{-2} \\ &\quad + \frac{3}{64} x_W x_L - \frac{3}{16} x_W x_L^2 x_H^{-1} + \frac{9}{64} x_W x_B - \frac{9}{16} x_W x_B^2 x_H^{-1} \end{aligned} \quad (113)$$



Theorem

Therefore *mass renormalization* has removed

all logarithms in the residue of the *simple ultraviolet pole* for the *fermionic part*

while a *non-local residue* remains in the *bosonic part*.

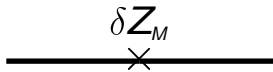
Unfortunately a simple procedure of *W mass renormalization* is not enough to get rid of *logarithmic residues in the bosonic component* and the reason is that in a *bosonic loop* we may have three different fields, the *W*, the ϕ and the *charged ghosts* and *only one mass* is available.



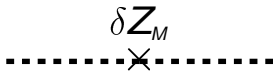
Example

The situation is illustrated in Fig. 3 where the cross denotes insertion of a counterterm δZ_M ; the latter is fixed to remove the ultraviolet pole in the W self-energy and one easily verifies that the total in the second and third line of Fig. 3 (ϕ and X self-energies, respectively) is not ultraviolet finite.

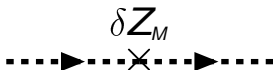




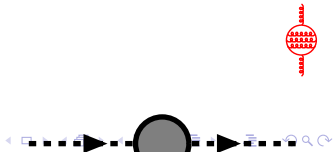
+

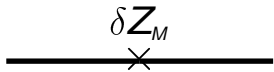


+

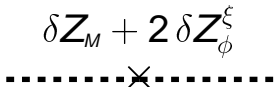


+

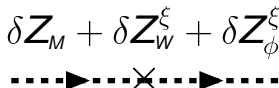




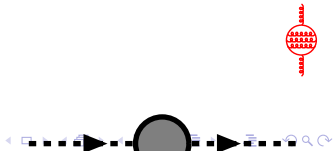
+



+



+



The procedure has to be **changed** if we want to make the result in the **bosonic sector** as similar as possible to the one in the **fermionic sector**. With this goal in mind we introduce the **following counterterms**

$$W_\mu = Z_W^{1/2} W_\mu^R, \quad \phi = Z_\phi^{1/2} \phi^R, \quad M_W = Z_M^{1/2} M_W^R. \quad (115)$$

Our solution is to work in a **$R_{\xi\xi}$ -gauge** where the **gauge-fixing term** (limited to the **charged sector**) is

$$\mathcal{C} = -\frac{1}{\xi_W} \partial_\mu W_\mu + \xi_\phi M_W \phi. \quad (116)$$



We also introduce **additional counter-terms** for the **gauge parameters**,

$$\xi_W = Z_W^\xi \xi_W^R, \quad \xi_\phi = Z_\phi^\xi \xi_\phi^R. \quad (117)$$

Our scheme is further specified by imposing the **condition**

$$\xi_W^R = \xi_\phi^R = 1. \quad (118)$$



Dropping from now on the index R for **renormalized fields** and **parameters** we define the **counter-Lagrangian** to be

$$\mathcal{L}_{\text{ct}} = \frac{g^2}{16\pi^2} \left[\mathcal{L}_{\text{ct}}^{WW} + \mathcal{L}_{\text{ct}}^{\phi W} + \mathcal{L}_{\text{ct}}^{\phi\phi} \right], \quad \mathcal{L}_{\text{ct}}^{ij} = \Phi_i^R \mathcal{O}_{ij} \Phi_i^R, \quad (119)$$

Φ_i being a **vector** or **scalar** field. We define **δZ factors** in the **MS -scheme** as

$$Z = 1 + \frac{g^2}{16\pi^2} \delta Z \frac{1}{\epsilon}, \quad (120)$$



and obtain

$$\begin{aligned}\epsilon \mathcal{O}_{\mu\nu}^{WW} &= - \left[\delta Z_W (p^2 + M_W^2) + \delta Z_M M_W^2 \right] \delta_{\mu\nu} + 2 \delta Z_W^\xi p_\mu p_\nu, \\ \epsilon \mathcal{O}^{\phi\phi} &= - \left[\delta Z_\phi (p^2 + M_W^2) + M_W^2 (\delta Z_M + 2 \delta Z_\phi^\xi) \right], \\ \epsilon \mathcal{O}_\mu^{W\phi} &= (\delta Z_W^\xi - \delta Z_\phi^\xi) i M_W p_\mu.\end{aligned}\tag{121}$$



These counter-terms are used to remove all poles from the transitions in the charged sector. After including the tadpole contribution and using Eq.(118) we find

$$\begin{aligned}
 \delta Z_W^\xi &= \frac{11}{6}, \\
 \delta Z_\phi^\xi &= -\frac{2}{3} + \frac{3}{2}c^{-4}x_H^{-1} - \frac{5}{4}c^{-2} + x_L - 2x_L^2x_H^{-1} \\
 &\quad + 3x_B - 6x_B^2x_H^{-1} + 3x_T - 6x_T^2x_H^{-1} + 3/4x_H + 3x_H^{-1}, \\
 \delta Z_W &= \frac{11}{3} \\
 \delta Z_\phi &= 2 + c^{-2} - x_L - 3x_B - 3x_T, \\
 \delta Z_M &= -\frac{2}{3} - 3c^{-4}x_H^{-1} + \frac{3}{2}c^{-2} - x_L + 4x_L^2x_H^{-1} - 3x_B \\
 &\quad + 12x_B^2x_H^{-1} - 3x_T + 12x_T^2x_H^{-1} - \frac{3}{2}x_H - 6x_H^{-1}. \tag{122}
 \end{aligned}$$



Theorem

An *important result* follows, namely *both*

$$-Z_W^{1/2} (\xi_W Z_W^\xi)^{-1}, \quad +Z_M^{1/2} Z_\phi^\xi Z_\phi^{1/2} M_{\xi\phi}, \quad (123)$$

are *ultraviolet finite* so that the *gauge-fixing term* remains *unrenormalized*.



To continue our derivation we consider the **ghost Lagrangian** and the associated **counter-terms**,

$$\mathcal{L}_g = Z_X \bar{X}^\pm \left[\frac{1}{Z_W^\xi \xi_W} \partial^2 - Z_\phi^\xi Z_M \xi_\phi M_W^2 \right] X^\pm. \quad (124)$$

To this **Lagrangian** corresponds an **operator**

$$\epsilon \mathcal{O}^{gg} = - \left[(\delta Z_X - \delta Z_W^\xi) (p^2 + M_W^2) + (\delta Z_M + \delta Z_W^\xi + \delta Z_\phi^\xi) M_W^2 \right]. \quad (125)$$



A simple calculation shows that, with the choice

$$\delta Z_X = \frac{23}{6}, \quad (126)$$

also the ghost Lagrangian is ultraviolet finite. The correct combination of mass counterterms is illustrated in Fig. 4. Note that in the \overline{MS} scheme we define

$$Z = 1 + \frac{g^2}{16\pi^2} \delta Z \left[-\frac{2}{\epsilon} + \Delta_{UV} \right], \quad \delta Z_{\overline{MS}} = -\frac{1}{2} \delta Z_{MS}. \quad (127)$$

Note that the two-loop part of Π remains unchanged since modifications are of $\mathcal{O}(g^6)$ while for $\Pi_{\text{bos}}^{(1)}$ we have to repeat the calculation, working in the new gauge.



The bare propagators for charged fields in the $R_{\xi\xi}$ gauge are

$$\begin{aligned}
 \bar{\Delta}_{\mu\nu}^{WW} &= \frac{1}{p^2 + M^2} \left[\delta_{\mu\alpha} + \frac{\xi_W^2 - 1}{p^2 + \xi_W^2 M^2} p_\mu p_\alpha \right] \\
 &\quad \times \left[\delta_{\alpha\nu} + \left(1 - \frac{\xi_\phi}{\xi_W}\right)^2 \frac{\xi_W^2 M^2}{(p^2 + \xi_W \xi_\phi M^2)^2} p_\alpha p_\nu \right], \\
 \bar{\Delta}_\mu^{W\phi} &= i M p_\mu \frac{\xi_W (\xi_\phi - \xi_W)}{(p^2 + \xi_W \xi_\phi M^2)^2}, \quad \bar{\Delta}^{\phi\phi} = \frac{p^2 + \xi_W^2 M^2}{(p^2 + \xi_W \xi_\phi M^2)^2}, \\
 \bar{\Delta}^{gg} &= \frac{\xi_W}{p^2 + \xi_W \xi_\phi M^2},
 \end{aligned} \tag{128}$$

where the last propagator refers to the ghost - ghost transition.



One example will be enough to **describe the procedure**. Consider the **following integral**, corresponding to a ϕ loop in the **AA self-energy**:

$$I_{\mu\nu} = \int d^n q \frac{(q^2 + \xi_W^2 M_W^2) ((q+p)^2 + \xi_W^2 M_W^2)}{(q^2 + \xi_W \xi_\phi M_W^2)^2 ((q+p)^2 + \xi_W \xi_\phi M_W^2)^2} \times (2q_\mu + p_\mu)(2q_\nu + p_\nu). \quad (129)$$

We expand **the propagators**,

$$\begin{aligned} (q^2 + \xi_W^2 M_W^2)^{-k} &= (q^2 + M_W^2)^{-k} \\ &\quad - 2k \frac{g^2}{16\pi^2 \epsilon} dZ_W^\xi M_W^2 (q^2 + M_W^2)^{-k-1} + \dots, \\ (q^2 + \xi_W \xi_\phi M_W^2)^{-k} &= (q^2 + M_W^2)^{-k} \\ &\quad - k \frac{g^2}{16\pi^2 \epsilon} (dZ_W^\xi + dZ_\phi^\xi) M_W^2 (q^2 + M_W^2)^{-k-1} + \dots \end{aligned} \quad (130)$$



and obtain

$$I_{\mu\nu} = I_0 \delta_{\mu\nu} + I_1 p_\mu p_\nu, \quad (131)$$

with **form factors**

$$\begin{aligned} I_0 &= I_0(\xi = 1) + i \pi^2 g^2 \Delta I_0 dZ_\phi^\xi, \\ \Delta I_0 &= \frac{1}{8} \frac{n-2}{n-1} A_0(1, M_W^2) - \frac{n-1}{2} M_W^2 B_0(1, 1, p^2, M_W, M_W) \\ &\quad + \frac{1}{4} \frac{1}{n-1} M_W^2 (p^2 + M_W^2) B_0(1, 2, p^2, M_W, M_W), \end{aligned} \quad (132)$$

where M_W is the **bare W mass**. Collecting all diagrams, **renormalizing** the **W mass** and inserting the solution for the **renormalization constants** we find the expression for the **bosonic, one-loop, AA self-energy**:



$$\Pi_{\text{bos}}^{(1)} \rightarrow \frac{6}{\epsilon} + 6 - 3\Delta_{UV} + 8x_W + \dots \quad (133)$$



Including both components and taking into account the additional contribution arising from renormalization we finally get residues for the ultraviolet poles which show the expected properties:

$$\begin{aligned} R^{(2)} &= -\frac{55}{768}, \\ R^{(1)} &= \frac{11}{192} \Delta_{UV} + \frac{1199}{27648} - \frac{131}{6912} c^{-2} + \frac{3}{512} x_L + \frac{13}{1536} x_T \\ &\quad + \frac{7}{1536} x_B. \end{aligned} \tag{134}$$

Eq.(134) shows complete cancellation of poles with a logarithmic residue; furthermore the two residues in Eq.(134) are scale independent and cancel in the difference $\Pi(p^2) - \Pi(0)$.



Transitions

A **final comment** concerns the **Z-photon transition** which is **not zero**, at $p^2 = 0$, in **any gauge** where $\xi \neq 1$ even after the Γ_1 **re-diagonalization procedure**.

However, in our case, the **non-zero result** shows up only due to a **different renormalization** of the two **bare gauge parameters** and it is, therefore, of $\mathcal{O}(g^4)$; it can be **absorbed** into Γ_2 which does not modify our result for Π since there are no Γ_2 -**dependent terms** in the **AA transition** (only Γ_1^2 appears).



renormalization procedure

One should observe that **our procedure** is completely **equivalent** to consider **one-loop diagrams** with the **insertion of one-loop counterterms** and one may wonder why

we have not included δZ_W , δZ_ϕ , δZ_X and also a δZ_e , arising from **charge renormalization** and a δZ_A from the **renormalization of the photon field**.



about counterterms

The argument goes as follows: **first** we consider the **relevant vertices** with **counterterms**:

$$\begin{aligned}AWW &= Z_W Z_A^{1/2} Z_e \otimes \text{Born}, \\A\phi\phi &= Z_\phi Z_A^{1/2} Z_e \otimes \text{Born}, \\AW\phi &= (Z_W Z_\phi Z_A Z_M)^{1/2} Z_e \otimes \text{Born}, \\A\bar{X}^\pm X^\pm &= Z_X Z_A^{1/2} Z_e \otimes \text{Born}.\end{aligned}\tag{135}$$



Next, we consider the **ultraviolet divergent part** of the corresponding **one-loop diagrams** and obtain:

$$V_{UV} = \frac{g^2}{16\pi^2} \frac{\delta V}{\epsilon}, \quad (136)$$

where

$$\begin{aligned} \delta V_{\alpha\beta\gamma}^{AWW} &= -\frac{11}{3} \delta_{\alpha\beta} (p_2 + 2p_1)_\gamma + \frac{11}{3} \delta_{\alpha\gamma} (p_1 + 2p_2)_\beta \\ &\quad + \frac{11}{3} \delta_{\beta\gamma} (p_1 - p_2)_\alpha \\ \delta V_\alpha^{A\phi\phi} &= (2 + c^{-2} - x_L - 3x_T - 3x_B) (p_1 - p_2)_\alpha, \\ \delta V_\alpha^{AXX} &= 2p_{1\alpha}, \\ \delta V_{\alpha\gamma}^{AW\phi} &= i\delta_{\alpha\gamma} M_W \left(\frac{3}{2}c^{-4} \frac{1}{x_H} - \frac{5}{4}c^{-2} - 2\frac{x_L^2}{x_H} - 6\frac{x_T^2}{x_H} - 6\frac{x_B^2}{x_H} + \frac{3}{x_H} + \frac{3}{4}x_H \right. \\ &\quad \left. + x_L + 3x_T + 3x_B - \frac{5}{2} \right). \end{aligned} \quad (137)$$



With these results we can prove that

$$\delta Z_e + \frac{1}{2} \delta Z_A = 0, \quad (138)$$

i.e. that, like in QED, charge renormalization is only due to vacuum polarization. Note that the Γ_1 prescription is crucial for proving the Ward identity of Eq.(138). Consider now the one-loop photon self-energy in our gauge; for instance, the diagrams with a ghost loop have vertices proportional to Z_x (thanks to Eq.(138)) and ghost propagators given by

$$\Delta^{gg} = \frac{1}{Z_x} \frac{\xi_w}{p^2 + \xi_w \xi_\phi m w^2}. \quad (139)$$

Clearly, δZ_x gives no contribution. The same holds for all other diagrams and for the remaining counterterms, δZ_ϕ and δZ_w . In conclusion, in computing Π we can forget about one-loop diagrams with field and charge counterterms and only worry about mass renormalization which we do, in some unconventional way, by expanding the explicit expression for $\Pi^{(1)}(s)$.



Inclusion of Δ_{UV}

In the previous section we have performed renormalization in the MS scheme and here we proceed by extending the same procedure to the \overline{MS} scheme. The counterterms in the two schemes are connected by the simple relation $\delta Z_{\overline{MS}} = -\frac{1}{2} \delta Z_{MS}$ and what we may show that not only the double and single ultraviolet poles of $\Pi(s)$ have scale independent, local, residues but also the terms proportional to powers of Δ_{UV} have the same property.



Fermion mass fitting equations

For the **complete answer** we need **fitting equations** that relate the **bare masses** to the **physical** ones since the **renormalized mass** is only an **intermediate parameter** which is bound to disappear in the expression for any physical observable. For a **generic $u - d$ doublet** we obtain

$$\begin{aligned} m_f &= m_f^{\text{phys}} + \frac{g^2}{16\pi^2} \Sigma_f \Big|_{m=m^{\text{phys}}}, \\ m_{f \text{ ren}}^2 &= m_{f \text{ phys}}^2 \left\{ 1 + \frac{g^2}{8\pi^2} \left[\frac{\Sigma_f}{m_f^2} \Big|_{m=m^{\text{phys}}} - \delta Z_m^f \right] \right\} \end{aligned} \quad (140)$$



W mass fitting equations

The relation between **renormalized** and **physical W mass** is

$$M_{W \text{ ren}}^2 = M_{W \text{ phys}}^2 \left\{ 1 + \frac{g^2}{16 \pi^2} \left[\frac{\text{Re} \Sigma_{WW}(-M_{W \text{ phys}}^2)}{M_{W \text{ phys}}^2} - \delta Z_M \right] \right\}, \quad (141)$$

where the quantity within **square brackets** is **ultraviolet finite** by construction and where

$$\Sigma_{WW} = \sum_{\text{gen}} \Sigma_{WW}^f + \Sigma_{WW}^b - 2(\beta_{t1} + \Gamma_1). \quad (142)$$



Definitions

Writing a renormalization equation that involves G_F should not be confused with making a prediction with the muon life-time.

In the following section we present few examples that are relevant in evaluating Δg (see Eq.(145)) up to two-loops and therefore in constructing one of our renormalization equations.

- The **Lagrangian** of the **Fermi theory** which is relevant for our purposes can be written as:

$$\mathcal{L}_F = \mathcal{L}_{QED} + \frac{G_F}{\sqrt{2}} \bar{\psi}_{\nu_{\mu}} \gamma^{\mu} \gamma_+ \psi_{\mu} \bar{\psi}_{\nu_e} \gamma^{\mu} \gamma_+ \psi_{\nu_e}, \quad (143)$$

where $\gamma_+ = 1 + \gamma_5$.



To leading order in G_F and to all orders in α the muon lifetime takes the form

$$\frac{1}{\tau_\mu} = \Gamma_0 (1 + \Delta g), \quad \Gamma_0 = \frac{G_F^2 m_\mu^5}{192 \pi^3}. \quad (144)$$

The standard model weak corrections to τ_μ are conventionally parametrized by the relation

$$\frac{G_F}{\sqrt{2}} = \frac{g^2}{8 M^2} (1 + \Delta g). \quad (145)$$

Our goal will be to derive an explicit expression for Δg so that one can use Eq.(145) as a relation where on the left hand side there is a quantity whose value is obtained by experiment and where on the right hand side we have bare quantities.



The quantity Δg may be written as the sum of various contributions, which are

$$\Delta g = \Delta g^{WF} + \Delta g^V + \Delta g^B + \Delta g^S. \quad (146)$$

The various terms arise from **wave-function renormalization** factors, **weak vertices**, **boxes** and the **W self-energy**. **Self-energy** corrections always play a special role and will be discussed separately, although they are crucial in establishing **gauge parameter independence**.



Strategy of the calculation

In the standard model and in the $\xi = 1$ gauge the lowest order amplitude is

$$\begin{aligned}\mathcal{M}_{SM;0} &= (2\pi)^4 i \frac{g^2}{8} \frac{1}{Q^2 + M^2} \bar{u}(p_{\nu_\mu}) \gamma^\alpha \gamma_+ u(p_\mu) \bar{u}(p_e) \gamma^\alpha \gamma_+ v(p_{\nu_e}) \\ &\approx \frac{G_F}{\sqrt{2}} \bar{u}(p_{\nu_\mu}) \gamma^\alpha \gamma_+ u(p_\mu) \bar{u}(p_e) \gamma^\alpha \gamma_+ v(p_{\nu_e}) \equiv \mathcal{M}_F,\end{aligned}\quad (147)$$

where we have introduced $Q = p_\mu - p_e$.



Note that at one loop we have

$$\frac{1}{\tau_\mu} = \frac{m_\mu^5}{192 \pi^3} \frac{g^4}{32 M^2} (1 + 2 \Delta g^{(1)} + \Delta q^{(1)}), \quad (148)$$

and we have to separate the **pure e.m. corrections** evaluated in the **Fermi theory** to obtain $\Delta g^{(1)}$. To obtain the amplitude which generates the one-loop weak correction we consider first

$$\mathcal{M}_{W;1} = \mathcal{M}_{SM;1} - \mathcal{M}_{\text{sub};1}, \quad (149)$$

where $\mathcal{M}_{\text{sub};1}$ is obtained by grouping the one-loop SM corrections with **one photon line connected to external fermions** and **one W line**, by shrinking the **W line to a point** and by replacing the corresponding **W propagator** with $1/M^2$.



At the one-loop level and after the substitution $g^2/(8 M^2) \rightarrow G_F/\sqrt{2}$ we obtain

$$\mathcal{M}_{\text{sub}; 1} \equiv \mathcal{M}_{F; 1}, \quad (150)$$

where the latter generates $\Gamma_0 \Delta q^{(1)}$. In the subtracted amplitude the **soft terms** have disappeared and we generate $\Delta g^{(1)}$ with the help of

$$\mathcal{M}_{W; 1}^{\text{leading}} = \lim_{p_i, m_j \rightarrow 0} \mathcal{M}_{\text{sub}; 1}, \quad (151)$$

i.e. we only retain the leading part, with **vanishing lepton masses** and **external momenta**, which amounts to neglect corrections of $\mathcal{O}(\alpha m^2/M^2)$. One-loop diagrams with **no photons** only have an **hard component** and do not need a subtraction.



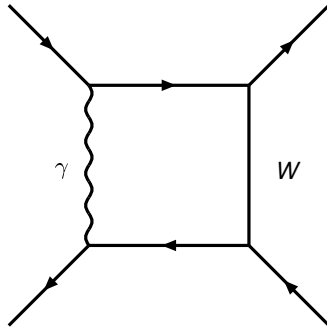


Figure: Infrared divergent one-loop box.



This amplitude contains **two structures**,

$$M_0 = \bar{u} \gamma^\alpha \gamma_+ u \bar{u} \gamma^\alpha \gamma_+ v, \quad M_1 = \bar{u} \gamma^\alpha \gamma^\mu \gamma^\beta \gamma_+ u \bar{u} \gamma^\beta \gamma^\mu \gamma^\alpha \gamma_+ v. \quad (152)$$

However, M_1 is simply related to the **current** \otimes **current** structure as it will be illustrated by considering the case of the one-loop box with W, γ exchange. We neglect for the moment all coupling constants and write

$$\mathcal{M}_{\text{box}, \gamma W}^{\text{sub}} = - \int d^n q \frac{q_\lambda q_\sigma}{(q^2 + M^2)(q^2)^2} J^{\alpha\lambda\beta} J^{\beta\sigma\alpha},$$

$$J^{\alpha\lambda\beta} = \bar{u}(p_{\nu_\mu}) \gamma^\alpha \gamma_+ \gamma^\lambda \gamma^\beta u(p_\mu), \quad J^{\beta\sigma\alpha} = \bar{u}(p_e) \gamma^\beta \gamma^\sigma \gamma^\alpha \gamma_+ v(p_{\nu_e}). \quad (153)$$



After integration we obtain

$$\mathcal{M}_{\text{box},\gamma W}^{\text{sub}} = -i \pi^2 B_0(2, 1; 0, 0, M) J^{\alpha\lambda\beta} J^{\beta\lambda\alpha}. \quad (154)$$

It can be shown that

$$J^{\alpha\lambda\beta} J^{\beta\lambda\alpha} = B^{(1)} M_0, \quad (155)$$

where $B^{(1)}$ is obtained with the help of a projection operator,



$$\sum_{\text{spin}} \mathcal{P} \left(\mathbf{J}^{\alpha\lambda\beta} \mathbf{J}^{\beta\lambda\alpha} - \mathbf{B}^{(1)} M_0 \right) = 0,$$

$$\mathcal{P} = \bar{v}(p_{\nu_e}) \gamma^\rho \gamma_+ u(p_{\nu_\mu}) \bar{u}(p_\mu) \gamma^\rho \gamma_+ u(p_e). \quad (156)$$

After a straightforward algebraic manipulation one obtains (in the limit $Q^2 \rightarrow 0$)

$$\mathbf{B}^{(1)} = (n - 2)^2, \quad (157)$$

which, after multiplication by $B_0(2, 1; 0, 0, M)$ and in the limit $n \rightarrow 4$ reproduces the correct result, proportional to $B_0(2, 1; 0, 0, M) - 1/2$.



Alternatively we start from the expression for the γ, W box without nullifying the soft scales,

$$\begin{aligned} \mathcal{M}_{\text{box}_{\gamma W}} &= \int d^q \frac{1}{d_0 d_1 d_2 d_3} \bar{u}(p_{\nu_\mu}) \gamma^\alpha \gamma_+ \left[-i (\not{q} + \not{p}_\mu) + m_\mu \right] \gamma^\beta u(p_\mu) \\ &\times \bar{u}(p_e) \gamma^\beta \left[-i (\not{q} + \not{p}_e) + m_e \right] \gamma^\alpha \gamma_+ v(p_{\nu_e}), \end{aligned} \quad (158)$$



where we introduce

$$d_0 = q^2, \quad d_1 = (q + p_\mu)^2 + m_\mu^2, \quad d_2 = (q + P)^2 + M^2, \quad d_3 = (q + p_e)^2 + m_e^2, \quad (159)$$

$$(p_\mu - p_{\nu_\mu})^2 = P^2, \quad (p_\mu - p_e)^2 = Q^2. \quad (160)$$

A **standard decomposition** gives

$$\frac{1}{d_0 d_1 d_2 d_3} = \frac{1}{P^2 + M^2} \left[\frac{1}{d_0 d_1 d_3} - \frac{1}{d_1 d_2 d_3} - 2 \frac{q \cdot P}{d_0 d_1 d_2 d_3} \right]. \quad (161)$$



- The **first term** in the decomposition (in the limit $|P^2| \ll M^2$) is the **QED vertex** in the **local Fermi theory** that can be computed with standard techniques;
- The **last two terms** inside the square bracket of Eq.(161) are **finite in the soft limit** so that the extra contribution from the infrared SM box can be evaluated for $m_\mu, m_e = 0$ and $Q^2, P^2 = 0$.

In this limit only the term with three propagators survives and gives the **well-known result**.

With this **technique** (**extracting** instead of **subtracting**) we circumvent the puzzling procedure of Eq.(151) where the subtracted term is zero in dimensional regularization. However, the two procedures are totally equivalent.



If we neglect, for the moment, issues related to **gauge parameter independence** it is convenient to define a **G constant** that is **totally process independent**,

$$\Delta g = \delta_G + \Delta g^S, \quad G = G_F \left(1 - \frac{g^2}{8 M^2} \delta_G \right), \quad \delta_G = \sum_{n=1} \left(\frac{g^2}{16 \pi^2} \right)^n \delta_G^{(n)}. \quad (162)$$

Alternatively, but always neglecting issues related to **gauge parameter independence**, we could resum δ_G by defining $G_R = G_F / (1 + \delta_G)$.



In one case we obtain

$$G = \frac{g^2}{8M^2} \left[1 - \frac{g^2}{16\pi^2 M^2} \Sigma_{WW}(0) \right]^{-1},$$
$$\Sigma_{WW}(0) = \Sigma_{WW}^{(1)}(0) + \frac{g^2}{16\pi^2} \Sigma_{WW}^{(2)}(0), \quad (163)$$

where Σ_{WW} is the W self-energy,



whereas **with resummation** we get

$$G_R = \frac{g^2}{8M^2} \left[1 - \frac{g^2}{16\pi^2 M^2} \bar{\Sigma}_{WW}(0) \right]^{-1},$$
$$\bar{\Sigma}_{WW}(0) = \Sigma_{WW}^{(1)}(0) + \frac{g^2}{16\pi^2} \left[\Sigma_{WW}^{(2)}(0) - \Sigma_{WW}^{(2)}(0) \delta_G^{(1)} \right]. \quad (164)$$



Part III

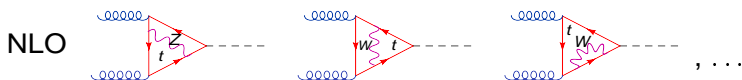
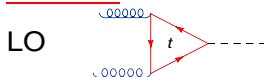
Lecture III



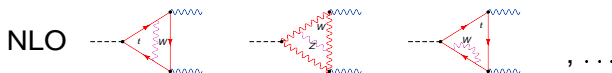
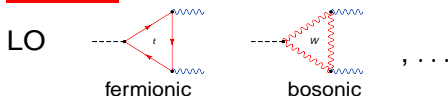
Calculation & Techniques

...some diagrams contributing to the EW 2-loop corrections

■ $gg \rightarrow H$:



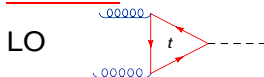
■ $H \rightarrow \gamma\gamma$:



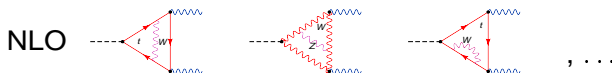
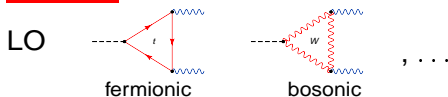
Calculation & Techniques

...some diagrams contributing to the EW 2-loop corrections

■ $gg \rightarrow H$:



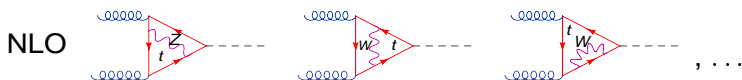
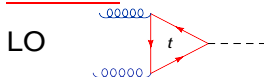
■ $H \rightarrow \gamma\gamma$:



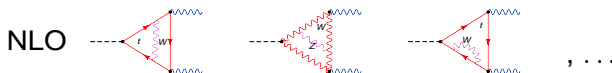
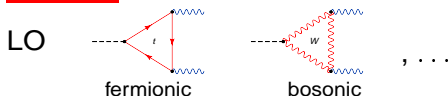
Calculation & Techniques

...some diagrams contributing to the EW 2-loop corrections

■ $gg \rightarrow H$:



■ $H \rightarrow \gamma\gamma$:



Calculation & Techniques

2-loop contributions are computed numerically:

- Diagrams: *GraphShot*

S. Actis, A. Ferroglia, G. Passarino, M. Passera, C.S., S. Uccirati

Form3 based package for automatic generation and manipulation of 1- and 2-loop Feynman diagrams:

insert Feynman-rules, perform traces, remove reducible scalar products, symmetrize integrals, reduction, counter terms, renormalization,...

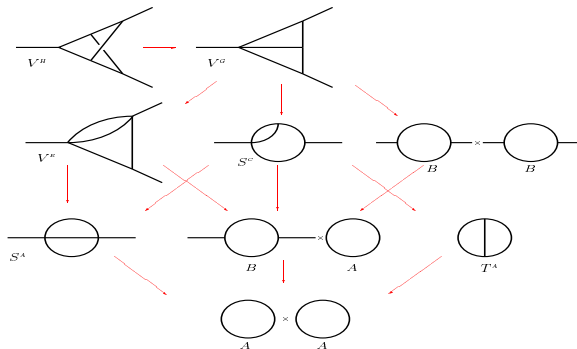
- \rightsquigarrow UV-finite integrals classified into:
 scalar, vector and tensor type integrals
 \rightsquigarrow mapped on form factors

- Form factors are evaluated numerically in parametric space

- Before num. integration: **Cancel collinear sing. + Study threshold**

For a moment consider $H \rightarrow \gamma\gamma$ without loss of generality

Generating the Amplitude: reduction



Recursive Reduction

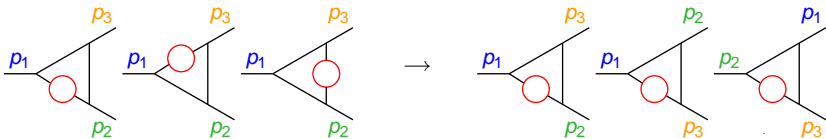
Generic child topologies of the V^H parent topology. The five-line V^G diagram is obtained by removing one line of the V^H diagram; the second line contains the child topologies of V^G (V^E , S^C and $B \times B$). The third line contains the topologies S^A , $B \times A$ and T^A , obtained by removing one line from the diagrams above. The arrows indicate the correspondences between parent and child topologies.



Generating the Amplitude

Strategy

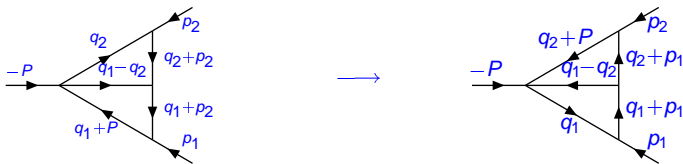
group diagrams into families, paying attention to permutation of external legs



Rooting

Strategy

mapping onto a standard rooting for loop momenta



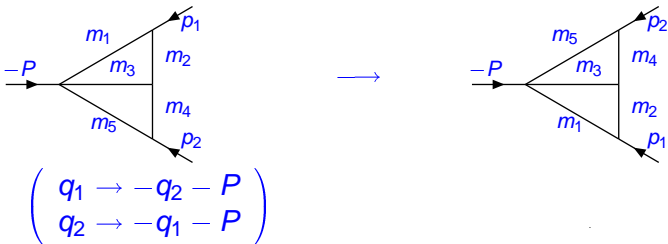
$$\begin{pmatrix} q_1 \rightarrow -q_1 - P \\ q_2 \rightarrow -q_2 - P \end{pmatrix}$$



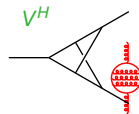
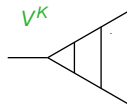
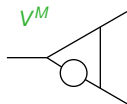
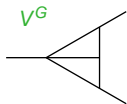
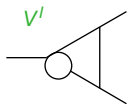
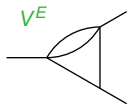
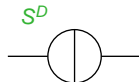
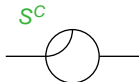
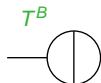
Symmetry

Strategy

apply symmetries to identify identical objects



List-of-diagrams: all what is needed



B

$$[f(q)] \xrightarrow{P} \text{circle} = \frac{\mu^\epsilon}{i\pi^2} \int d^n q \frac{f(q)}{[1][2]}, \quad \text{with} \quad \begin{cases} [1] = q^2 + m_1^2 \\ [2] = (q + P)^2 + m_2^2 \end{cases}$$

C

$$[f(q)] \xrightarrow{-P} \text{triangle} = \frac{\mu^\epsilon}{i\pi^2} \int d^n q \frac{f(q)}{[1][2][3]}, \quad \text{with} \quad \begin{cases} [1] = q^2 + m_1^2 \\ [2] = (q + p_1)^2 + m_2^2 \\ [3] = (q + P)^2 + m_3^2 \end{cases}$$



A Self-energies, vertices and tadpoles

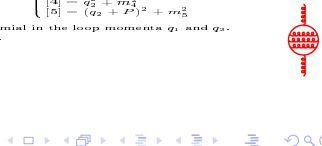
In this section we collect our conventions for the diagrams involved in the paper.

$$\begin{aligned}
 [f(q)] \xrightarrow{P} \text{Diagram B} &= \frac{\mu^\epsilon}{i\pi^2} \int d^n q \frac{f(q)}{[1][2]}, \quad \text{with } \begin{cases} [1] = q^2 + m_1^2 \\ [2] = (q + P)^2 + m_2^2 \end{cases} \\
 [f(q)] \xrightarrow{-P} \text{Diagram C} &= \frac{\mu^\epsilon}{i\pi^2} \int d^n q \frac{f(q)}{[1][2][3]}, \quad \text{with } \begin{cases} [1] = q^2 + m_1^2 \\ [2] = (q + p_1)^2 + m_2^2 \\ [3] = (q + P)^2 + m_3^2 \end{cases}
 \end{aligned}$$

Figure 25: The one-loop self-energy and vertex. f is a generic polynomial in the loop momentum q . The dimension of the space-time is $n = 4 - \epsilon$ and μ is the renormalization scale.

$$\begin{aligned}
 [f(q_1, q_2)] \xrightarrow{P} \text{Diagram 1} &= \frac{\mu^{2\epsilon}}{\pi^4} \int d^n q_1 d^n q_2 \frac{f(q_1, q_2)}{[1][2][3]}, \quad \text{with } \begin{cases} [1] = q_1^2 + m_1^2 \\ [2] = (q_1 - q_2)^2 + P^2 + m_2^2 \\ [3] = q_2^2 + m_3^2 \end{cases} \\
 [f(q_1, q_2)] \xrightarrow{P} \text{Diagram 2} &= \frac{\mu^{2\epsilon}}{\pi^4} \int d^n q_1 d^n q_2 \frac{f(q_1, q_2)}{[1][2][3][4]}, \quad \text{with } \begin{cases} [1] = q_1^2 + m_1^2 \\ [2] = (q_1 - q_2)^2 + m_2^2 \\ [3] = q_2^2 + m_3^2 \\ [4] = (q_2 + P)^2 + m_4^2 \end{cases} \\
 [f(q_1, q_2)] \xrightarrow{P} \text{Diagram 3} &= \frac{\mu^{2\epsilon}}{\pi^4} \int d^n q_1 d^n q_2 \frac{f(q_1, q_2)}{[1][2][3][4][5]}, \quad \text{with } \begin{cases} [1] = q_1^2 + m_1^2 \\ [2] = (q_1 - q_2)^2 + m_2^2 \\ [3] = q_2^2 + m_3^2 \\ [4] = (q_2 + P)^2 + m_4^2 \\ [5] = q_2^2 + m_5^2 \end{cases} \\
 [f(q_1, q_2)] \xrightarrow{P} \text{Diagram 4} &= \frac{\mu^{2\epsilon}}{\pi^4} \int d^n q_1 d^n q_2 \frac{f(q_1, q_2)}{[1][2][3][4][5]}, \quad \text{with } \begin{cases} [1] = q_1^2 + m_1^2 \\ [2] = (q_1 + P)^2 + m_2^2 \\ [3] = (q_1 - q_2)^2 + m_3^2 \\ [4] = q_2^2 + m_4^2 \\ [5] = (q_2 + P)^2 + m_5^2 \end{cases}
 \end{aligned}$$

Figure 26: The irreducible two-loop self-energies diagrams. f is a generic polynomial in the loop momenta q_1 and q_2 . The dimension of the space-time is $n = 4 - \epsilon$ and μ is the renormalization scale.



$$\begin{aligned}
[f(q_1, q_2)]_{V^\nu} &= \frac{\mu^{2\epsilon}}{\pi^4} \int d^n q_1 d^n q_2 \frac{f(q_1, q_2)}{[1][2][3][4]}, \quad \text{with} \quad \begin{cases} [1] = q_1^2 + m_1^2 \\ [2] = (q_1 - q_2)^2 + m_2^2 \\ [3] = (q_2 + p_2)^2 + m_3^2 \\ [4] = (q_2 + F)^2 + m_4^2 \end{cases} \\
[f(q_1, q_2)]_{V^\tau} &= \frac{\mu^{2\epsilon}}{\pi^4} \int d^n q_1 d^n q_2 \frac{f(q_1, q_2)}{[1][2][3][4][5]}, \quad \text{with} \quad \begin{cases} [1] = -q_1^2 + m_1^2 \\ [2] = (q_1 - q_2)^2 + m_2^2 \\ [3] = -q_2^2 + m_3^2 \\ [4] = (q_2 + p_1)^2 + m_4^2 \\ [5] = (q_2 + F)^2 + m_5^2 \end{cases} \\
[f(q_1, q_2)]_{V^\sigma} &= \frac{\mu^{2\epsilon}}{\pi^4} \int d^n q_1 d^n q_2 \frac{f(q_1, q_2)}{[1][2][3][4][5]}, \quad \text{with} \quad \begin{cases} [1] = -q_1^2 + m_1^2 \\ [2] = (q_1 - q_2)^2 + m_2^2 \\ [3] = -q_2^2 + m_3^2 \\ [4] = (q_2 + p_1)^2 + m_4^2 \\ [5] = (q_2 + F)^2 + m_5^2 \end{cases} \\
[f(q_1, q_2)]_{V^\rho} &= \frac{\mu^{2\epsilon}}{\pi^4} \int d^n q_1 d^n q_2 \frac{f(q_1, q_2)}{[1][2][3][4][5]}, \quad \text{with} \quad \begin{cases} [1] = -q_1^2 + m_1^2 \\ [2] = (q_1 + p_1)^2 + m_2^2 \\ [3] = (q_1 - q_2)^2 + m_3^2 \\ [4] = (q_2 + p_1)^2 + m_4^2 \\ [5] = (q_2 + F)^2 + m_5^2 \end{cases} \\
[f(q_1, q_2)]_{V^\kappa} &= \frac{\mu^{2\epsilon}}{\pi^4} \int d^n q_1 d^n q_2 \frac{f(q_1, q_2)}{[1][2][3][4][5][6]}, \quad \text{with} \quad \begin{cases} [1] = -q_1^2 + m_1^2 \\ [2] = (q_1 + F)^2 + m_2^2 \\ [3] = (q_1 - q_2)^2 + m_3^2 \\ [4] = -q_2^2 + m_4^2 \\ [5] = (q_2 + p_1)^2 + m_5^2 \\ [6] = (q_2 + F)^2 + m_6^2 \end{cases} \\
[f(q_1, q_2)]_{V^\eta} &= \frac{\mu^{2\epsilon}}{\pi^4} \int d^n q_1 d^n q_2 \frac{f(q_1, q_2)}{[1][2][3][4][5][6]}, \quad \text{with} \quad \begin{cases} [1] = -q_1^2 + m_1^2 \\ [2] = (q_1 - p_2)^2 + m_2^2 \\ [3] = (q_1 - q_2 + p_1)^2 + m_3^2 \\ [4] = (q_1 - q_2 - p_2)^2 + m_4^2 \\ [5] = -q_2^2 + m_5^2 \\ [6] = (q_2 - p_1)^2 + m_6^2 \end{cases}
\end{aligned}$$

Figure 27: The irreducible two-loop vertex diagrams. f is a generic polynomial in the loop momenta q_1 and q_2 . The dimension of the space-time is $n = 4 - \epsilon$ and μ is the renormalization scale.

B Properties of projectors

In this appendix we briefly summarize a general approach based on the work of Ref. [52]. Amplitudes for two-loop $1 \rightarrow 2$ processes are decomposed into form factors which have to be extracted with proper projection operators. Let us consider tensor, one-loop, N -point functions in n dimensions ($N \leq 5$, $n = 4 - \epsilon$)

$$S_{NN}^{\mu\nu} = \frac{\mu^\epsilon}{i\pi^2} \int d^n q \frac{q^\mu \cdots q^\nu}{\prod_{i=0, N-1}^n(t_i)}, \quad (i) = (q + p_1 + \cdots + p_i)^2 + m_i^2, \quad (234)$$

Any Feynman diagram G with L internal legs and l loops is representable in n dimensions as

$$G = (i\pi^{n/2})^l \Gamma\left(L - \frac{n}{2}l\right) \int \frac{dx_G \delta(1 - x_G)}{U^{n/2} (V - i0)^{L - n l / 2}}, \quad (165)$$

where Γ is the Euler gamma-function and where the integration measure can be written as

$$dx_G = \prod_{i=1}^l dx_i, \quad x_G = \sum_{i=1}^l x_i. \quad (166)$$

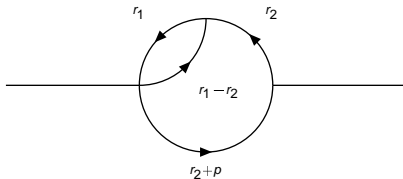


Furthermore, the polynomials V and U are defined by

$$V = \sum_i m_i^2 x_i + \sum_i q_i^2 x_i - \frac{1}{U} \sum_{ij} B_{ij} q_i \cdot q_j x_i x_j,$$

$$U = \sum_T \prod_{x_i \in T} x_i = \det(U_{rs}), \quad U_{rs} = \sum_i x_i \eta_{ir} \eta_{is}, \quad (167)$$

where η_{is} is the projection of line i along the loop s . Furthermore, T is a co-tree and B_{ij} are the parametric functions for the given diagram. Although these functions can be determined completely by the topological structure of the diagram G we give a practical example of how to construct U and V for the two-loop diagram of Fig. 2



After introducing Feynman parameters the integrand contains a factor $1/D^4$ with

$$D = \sum_{i=1}^4 x_i (q_i^2 + m_i^2), \quad q_1 = r_1, \quad q_2 = r_1 - r_2, \quad q_3 = r_2, \quad q_4 = r_2 + p, \quad (168)$$

where r_s is the independent integration momentum around the loop s , x_i are Feynman parameters with $\sum_i x_i = 1$. The part of D which is quadratic in $r_{1,2}$ will be written as

$$r^t U r, \quad U_{11} = x_1 + x_2, \quad U_{22} = x_2 + x_3 + x_4, \quad U_{12} = U_{21} = -x_2. \quad (169)$$

Next we rewrite U_{ij} as a sum,

$$U_{ij} = \sum_{l=1}^4 \eta_{il} \eta_{lj} x_l, \quad (170)$$

and derive the coefficients η as

$$\eta_{11} = \eta_{21} = \eta_{32} = \eta_{42} = +1, \quad \eta_{22} = -1, \quad \eta_{31} = \eta_{41} = \eta_{12} = 0. \quad (171)$$



Furthermore, let U be the determinant of the matrix U_{ij} , thus

$$U = \det (U_{ij}) = x_1 x_{234} + x_2 x_{34}, \quad (172)$$

where $x_{ij\dots l} = x_i + x_j + \dots + x_l$. Momenta p_i will then be defined with $p_4 = p$ and $p_i = 0$ for $i < 4$. The following change of variables in the r_1 -integral is then performed:

$$r_1^\mu \rightarrow r_1^\mu - \sum_{j=1}^4 \sum_{t=1}^2 x_j p_j^\mu \eta_{it} (U^{-1})_{1t} = r_1^\mu - \sum_{t=1}^2 x_4 p^\mu \eta_{4t} (U^{-1})_{1t} = r_1^\mu - x_4 \frac{x_2}{U} p^\mu. \quad (173)$$

Similarly we change variable also in the r_2 -integral,

$$r_2^\mu \rightarrow r_2^\mu - \sum_{j=1}^4 \sum_{r=1}^2 x_j p_j^\mu \eta_{jr} (U^{-1})_{2r} = r_2^\mu - x_4 \frac{x_{12}}{U} p^\mu. \quad (174)$$



We derive the following result:

$$\sum_{i=1}^4 x_i (q_i^2 + m_i^2) \rightarrow r^t U r + V, \quad (175)$$

which defines the polynomial V as

$$V = \sum_{i=1}^4 x_i m_i^2 + x_4 p^2 - \frac{1}{U} x_{12} x_4^2 p^2. \quad (176)$$

After a diagonalization of the symmetric matrix U ,

$$\sum_{i'j'} (A^{-1})_{ii'} U_{i'j'} A_{j'l} = U_i \delta_{ij}, \quad (177)$$

we perform a change of variables with unit Jacobian, $s_i = \sum_j A_{ij} f_j$, and use

$$\begin{aligned} \int \prod_{i=1}^l ds_i \left[\sum_{i=1}^l U_i s_i^2 + V \right]^{-N_L} &= \int \prod_{i=2}^l ds_i ds_1 \left[U_1 s_1^2 + \sum_{i=2}^l U_i s_i^2 + V \right]^{-N_L} \\ &= i \pi^{n/2} U_1^{-n/2} \frac{\Gamma(N_L - n/2)}{\Gamma(N_L)} \int \prod_{i=2}^l ds_i \left[\sum_{i=2}^l U_i s_i^2 + V \right]^{n/2 - N_L} = \text{etc.}, \end{aligned} \quad (178)$$



to obtain the result of Eq.(165). Note that UV-singularities come from U . We also define

$$\bar{V} = U \left[\sum_i m_i^2 x_i + \sum_i q_i^2 x_i \right] - \sum_{ij} B_{ij} q_i \cdot q_j x_i x_j \quad (179)$$

and obtain

$$G = (i\pi^{n/2})^l \Gamma \left(L - \frac{n}{2} l \right) \int \frac{dx_G \delta(1 - x_G)}{U^{(n/2+1)l-L} (\bar{V} - i0)^{L-n/2l}}. \quad (180)$$



All-you-can-do-analytic

rule-of-the-game

Adelante Numerics, cum iudicio

UV

- UV poles, of course
- beware, *overlapping divergencies*

IR/Coll

- IR poles, of course
- Collinear logs, of course

upshot

Cancellations, if any, enforced analytically



All-you-can-do-analytic

rule-of-the-game

Adelante Numerics, cum iudicio

UV

- UV poles, of course
- beware, *overlapping divergencies*

IR/Coll

- IR poles, of course
- Collinear logs, of course

upshot

Cancellations, if any, enforced analytically



Collinear

Example

double divergency \rightsquigarrow double subtraction

$$\int_0^1 dx dy \frac{1}{xyA(x,y) + \lambda B(x,y)} = \int_0^1 dx dy \left\{ \frac{1}{xyA(x,y) + \lambda B(x,y)} \Big|_{++} + \frac{1}{xyA(x,0) + \lambda B(x,0)} \Big|_+ + \frac{1}{xyA(0,y) + \lambda B(0,y)} \Big|_+ + \frac{1}{xyA(0,0) + \lambda B(0,0)} \right\}, \quad \lambda \rightarrow 0$$

- First term \rightarrow set $\lambda = 0$
- Second (third) term \rightarrow integrate in $y(x) \rightsquigarrow \ln \lambda$
- Last term \rightarrow integrate in x and $y \rightsquigarrow \ln^2 \lambda$



Extracting Collinear divergencies

Theorem

Coefficients of collinear logarithms are integrals of one-loop functions

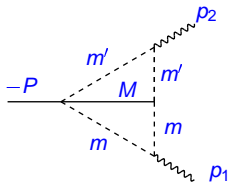
$$\begin{array}{c}
 \text{Diagram 1: Triangle with vertices } M_3, M_4, M_5, \text{ external momenta } -P, p_2, p_1, \text{ and a dashed line of mass } m. \\
 \text{Diagram 2: Triangle with vertices } M_3, M_4, M_5, \text{ external momenta } -P, p_2, \text{ and a wavy line of mass } m \text{ with momenta } (1-y)p_1 \text{ and } yp_1. \\
 \text{Diagram 3: Small diagram above showing a wavy line splitting into two dashed lines of mass } m.
 \end{array}$$

$$\text{Diagram 1} = \ln \frac{m^2}{s} \int_0^1 dy \text{Diagram 2} + \text{finite part}$$

Extracting Collinear divergencies

Example

Sometimes the answer is explicit



$$\begin{aligned}
 &= \ln \frac{m^2}{s} \ln \frac{m'^2}{s} \text{Li}_2 \left(\frac{s}{M^2} \right) + \left(\ln \frac{m^2}{s} + \ln \frac{m'^2}{s} \right) \\
 &\quad \left[\text{Li}_3 \left(\frac{s}{M^2} \right) + 2 S_{12} \left(\frac{s}{M^2} \right) \right. \\
 &\quad \left. - \ln \frac{M^2}{s} \text{Li}_2 \left(\frac{s}{M^2} \right) \right] + \text{finite part}
 \end{aligned}$$



General results I

Coll. behavior of
arbitrary two-loop
 q -scalar, UV-finite
diagrams

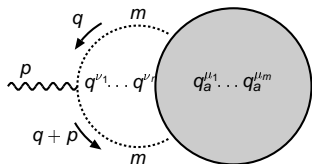
The diagrammatic equation shows the collinear limit of a two-loop q -scalar diagram. On the left, a wavy line with momentum p enters a grey circular blob labeled $q_a^{\mu_1} \dots q_a^{\mu_m}$. Two dashed lines with mass m form a loop, with momenta q and $q+p$ indicated. On the right, the same blob is shown with two external wavy lines: one with momentum zp and another with momentum $(1-z)p$. The equation is:

$$\text{Diagram} = \ln \frac{m^2}{s} \int_0^1 dz \text{Diagram} + \text{coll. fin.}$$



General results II

Generalization to
tensor integrals



$$= \ln \frac{m^2}{s} \left[1 - \frac{\epsilon}{2} \Delta_{\mathcal{W}}(s) - \frac{\epsilon}{4} \ln \frac{m^2}{s} \right]$$

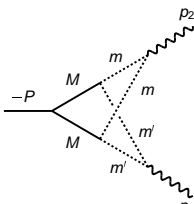
$$\times \int_0^1 dz (-z)^r (1-z)^r \text{ (diagram)} p^{\nu_1} \dots p^{\nu_r} + \text{c. f.}$$

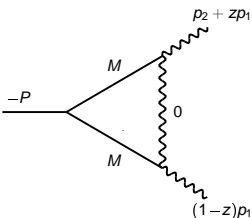

A Feynman diagram showing a scalar loop (grey circle) with internal mass m and internal indices $q_a^{\mu_1} \dots q_a^{\mu_m}$. Two wavy external lines enter from the top and bottom, with momenta zp and $(1-z)p$ respectively. The loop is labeled with $q_a^{\mu_1} \dots q_a^{\mu_m}$ at the vertex.



General results III

$$\omega = -P^2/M^2, \quad l_\omega = \ln(1 - \omega)$$

$$V_{\text{dc}}^H = [P^2 M^2 + 2P^2 q_1 \cdot p_1 - 4(q_1 \cdot p_1)^2]^{-P} \text{Diagram} = 2 \left(1 - \frac{1+\omega}{\omega} l_\omega\right) L L' + 2 \left[1 + \frac{1+\omega}{\omega} l_\omega (l_\omega - 1) + \text{Li}_2(\omega)\right] (L + L')$$


$$- 2 \int_0^1 dz [(1-z)P^2 L + (P^2 + 2q \cdot p_2) L']^{-P} \text{Diagram} + \text{Diagram}$$



Extracting Ultraviolet divergencies

$$\begin{aligned}
 V^I &= \text{Diagram} = \frac{1}{\pi^4} \int \frac{d^n q_1 d^n q_2}{\underbrace{[1][2][3][4][5]}_x}, \\
 &= C_\epsilon \int_0^1 dx \int dS_3(y_1, y_2, y_3) [x(1-x)]^{-\epsilon/2} (1-y_1)^{\epsilon/2-1} V^{-1-\epsilon}
 \end{aligned}$$

[1] = $q_1^2 + m_1^2$
 [2] = $(q_1 - q_2)^2 + m_2^2$
 [3] = $q_2^2 + m_3^2$
 [4] = $(q_2 + p_1)^2 + m_4^2$
 [5] = $(q_2 + P)^2 + m_5^2$

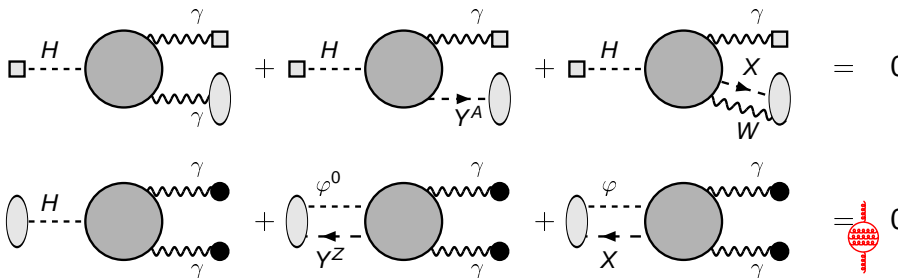
The **single pole** can always be expressed in terms of **1L**.

$$V^I = \text{Diagram} \times \text{Diagram} + \text{finite part.}$$



Checks

Off-shell WSTIs involving special sources; contracted sources
 → black circles, physical ones → gray boxes



Tasting numerical evaluation

Finite parts

Write the **finite part** of a FD in one of the following forms:

- 1 $\int dx \frac{Q(x)}{V(x)} \quad V(x) > 0;$
- 2 $\int dx Q(x) \ln^n V(x);$
- 3 $\int dx \frac{Q(x)}{V(x)} f\left(\frac{V(x)}{P(x)}\right) \quad f(x) = \ln^n(1+x), Li_n(x), S_{n,p}(x)$

Typical integrand with k Feynman variables:

$$z_1^{n_1} \cdots z_k^{n_k} V^\mu(z_1, \dots, z_k) \ln^m V(z_1, \dots, z_k),$$
$$\mu = -1, -2, \quad \{z\} \subseteq [0, 1]^k$$

V quadratic with respect to a subset of $\{z\}$ in which each z_i^2 is proportional to one squared external momentum.



bite-and-run strategy I

Multivariate Polylogs

- V is not complete
 - $\mu = -1$ and $m = 0$ ($m > 0$ similar)

$$\frac{1}{ax + b} = \partial_x \frac{1}{a} \ln \left(1 + \frac{a}{b} x \right)$$

- $\mu = -2$ and $m = 0$ ($m > 0$ similar)

$$\frac{1}{(axy + bx + cy + d)^2} = -\frac{\partial_x \partial_y}{ad - bc} \\ \times \ln \left\{ 1 + \frac{(ad - bc)x}{b(axy + bx + cy + d)} \right\}$$



bite-and-run strategy II

Multivariate PolyLogs

- V is complete

$$\begin{aligned}V(z) &= z^t H z + 2 K^t z + L = (z^t - Z^t) H (z - Z) + B \\ &= Q(z) + B,\end{aligned}$$

$$Z = -K^t H^{-1}, \quad B = L - K^t H^{-1} K,$$

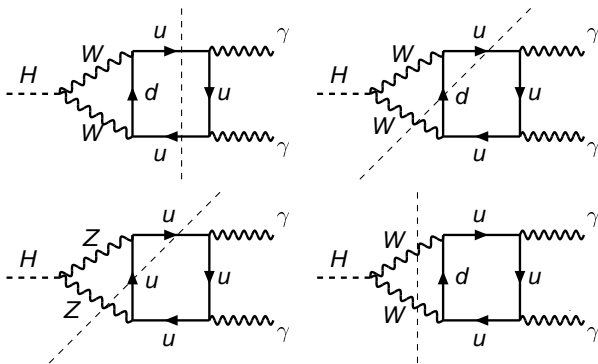
$$\mathcal{P}^t \partial_z Q(z) = -Q(z), \quad \mathcal{P} = -(z - Z)/2,$$

$$V^\mu(z) = (\beta - \mathcal{P}^t \partial_z) \int_0^1 dy y^{\beta-1} [Q(z) y + B]^\mu$$

$$\text{e.g. } V^{-1} = (1 - \mathcal{P}^t \partial_z) \frac{1}{Q} \ln \left(1 + \frac{Q}{B} \right)$$



Around threshold

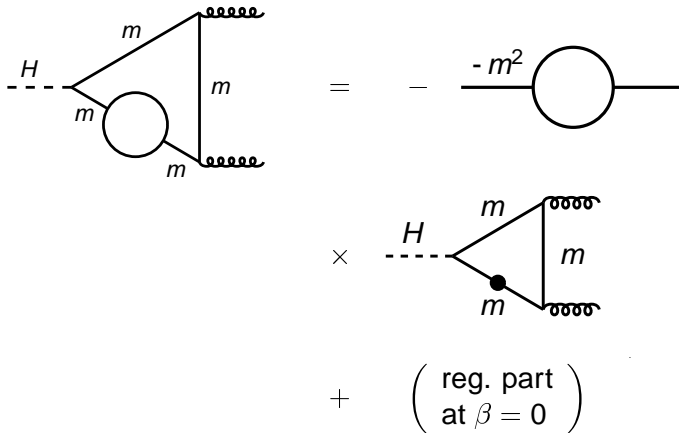


Singularities

- **FD** have a complicated analytical structure
- A frequently encountered singular behavior is associated with the so-called **normal thresholds**: the leading Landau singularities of self-energy-like diagrams
- which can appear, in more complicated diagrams, as **sub-leading singularities**.



$1/\beta$ -behavior



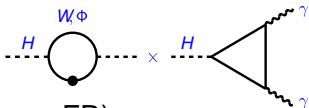
The diagram shows an equation for the $1/\beta$ behavior of a Feynman diagram. On the left is a triangle diagram with a dashed external line labeled H on the left. The top-left side is a solid line labeled m . The bottom-left side is a solid line labeled m that contains a circle loop. The right side is a solid vertical line labeled m . The top and bottom right corners of the triangle are connected to external lines with wavy patterns. This is followed by an equals sign and a minus sign, then a circle loop with a horizontal line passing through its center, labeled $-m^2$. Below this is a multiplication sign followed by a triangle diagram similar to the first one, but with a solid dot on the bottom-left side labeled m . This is followed by a plus sign and a large parenthesis containing the text "reg. part" and "at $\beta = 0$ ".

$$\begin{aligned} & \text{Triangle diagram with } H \text{ and } m \text{ lines, and a loop on the bottom-left side} \\ &= -m^2 \text{ (circle loop)} \\ &\times \text{ Triangle diagram with } H \text{ and } m \text{ lines, and a dot on the bottom-left side} \\ &+ \left(\begin{array}{l} \text{reg. part} \\ \text{at } \beta = 0 \end{array} \right) \end{aligned}$$

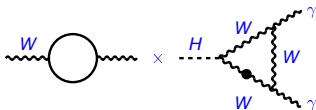


Origin of $1/\beta$

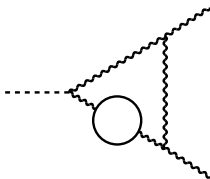
- (1-loop diagrams) \otimes (H wave-function FR)



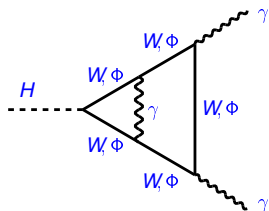
- (1-loop diagrams) \otimes (W mass FR)



- Pure 2-loop diagrams

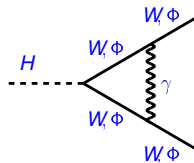


Logarithmic singularities



$\sim \ln \beta_w$

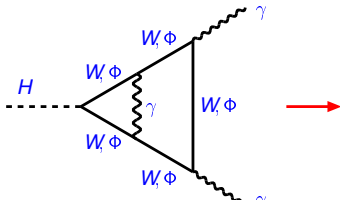
Remnant of
Coulomb
singularity



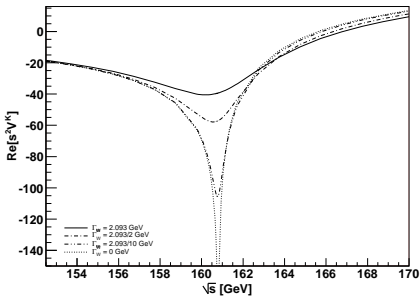
$\sim 1/\beta_w$

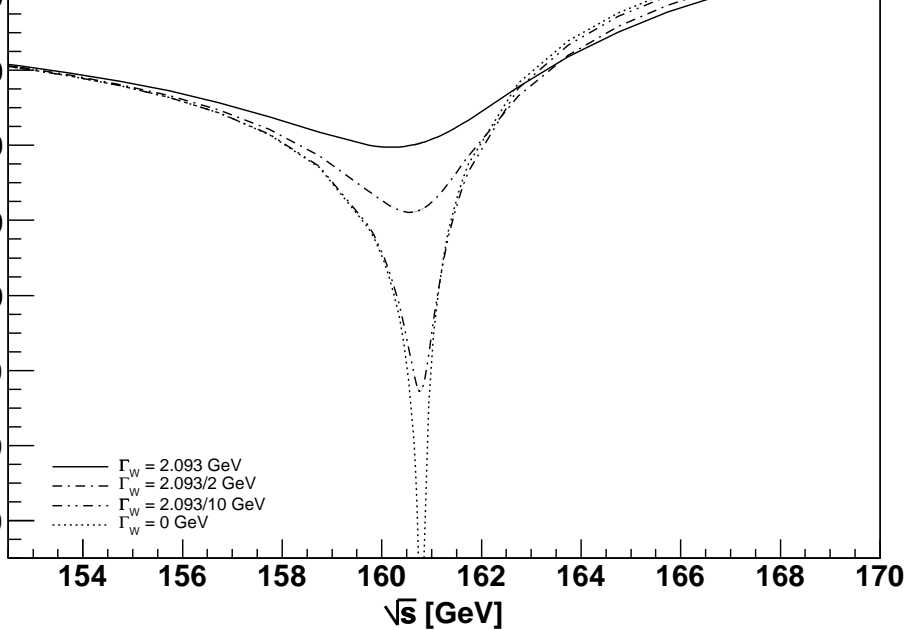


Cure for logarithmic singularities



Complex W Mass





Solutions

RM scheme - none

- where masses are the **real on-shell** ones; it gives the extension of the generalized minimal subtraction scheme up to two loop level.

MCM scheme - minimal

- start by removing the Re label in those terms that, coming from finite renormalization, **violate WSTIs**.
- split the amplitude

$$\mathcal{A}^{\text{NLO}} = \sum_{i=W,Z} \frac{A_{\text{SR},i}}{\beta_i} + A_{\text{LOG}} \ln \left(-\beta_W^2 - i0 \right) + A_{\text{REM}},$$



Solutions

RM scheme - none

- where masses are the **real on-shell** ones; it gives the extension of the generalized minimal subtraction scheme up to two loop level.

MCM scheme - minimal

- start by removing the Re label in those terms that, coming from finite renormalization, **violate WSTIs**.
- split the amplitude

$$\mathcal{A}^{\text{NLO}} = \sum_{i=W,Z} \frac{A_{\text{SR},i}}{\beta_i} + A_{\text{LOG}} \ln \left(-\beta_W^2 - i0 \right) + A_{\text{REM}},$$



Solutions

MCM scheme - minimal

- After proving that all coefficients, gauge-parameter independent by construction, **satisfy the WST identities**, we minimally modify the amplitude introducing the complex-mass scheme of for the **divergent terms**.

$$m_i^2 = M_i^2 \left[1 + \frac{G_F M_W^2}{2\sqrt{2} \pi^2} \operatorname{Re} \Sigma_i^{(1)}(M_i^2) \right] \Rightarrow$$

$$m_i^2 = s_i \left[1 + \frac{G_F s_W}{2\sqrt{2} \pi^2} \Sigma_i^{(1)}(s_i) \right],$$



Solutions

pitfalls

A nice feature of the MCM scheme is its simplicity

MCM scheme - minimal

- The MCM, however, does not deal with **cusps** associated with the crossing of normal thresholds.

MCM scheme - minimal

- The large and artificial effects arising around normal thresholds in the MCM scheme (or in RM scheme) are aesthetically unattractive.
- In addition, they represent a concrete problem in **assessing the impact** of two-loop EW corrections on processes relevant for the LHC.



Solutions

pitfalls

A nice feature of the MCM scheme is its simplicity

MCM scheme - minimal

- The MCM, however, does not deal with **cusps** associated with the crossing of normal thresholds.

MCM scheme - minimal

- The large and artificial effects arising around normal thresholds in the MCM scheme (or in RM scheme) are aesthetically unattractive.
- In addition, they represent a concrete problem in **assessing the impact** of two-loop EW corrections on processes relevant for the LHC.



Solutions

CM scheme - complete

- The procedure described for the **divergent terms** has been extended to the **remainder** A_{REM} . In particular, all **two-loop** diagrams have been computed with **complex masses** for the internal vector bosons.

CM scheme - complete

- In the full CM setup, the real parts of the W and Z self-energies induced by one-loop renormalization of the masses and the couplings have to be traded for the associated complex expressions.



Solutions

CM scheme - complete

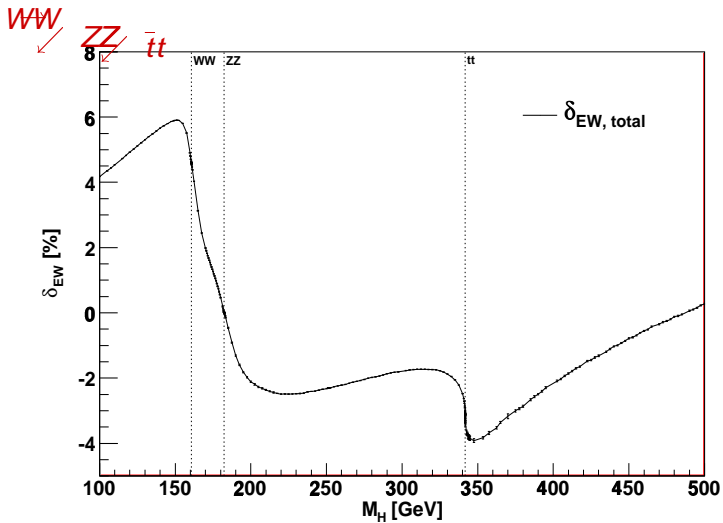
- The procedure described for the **divergent terms** has been extended to the **remainder** A_{REM} . In particular, all **two-loop** diagrams have been computed with **complex masses** for the internal vector bosons.

CM scheme - complete

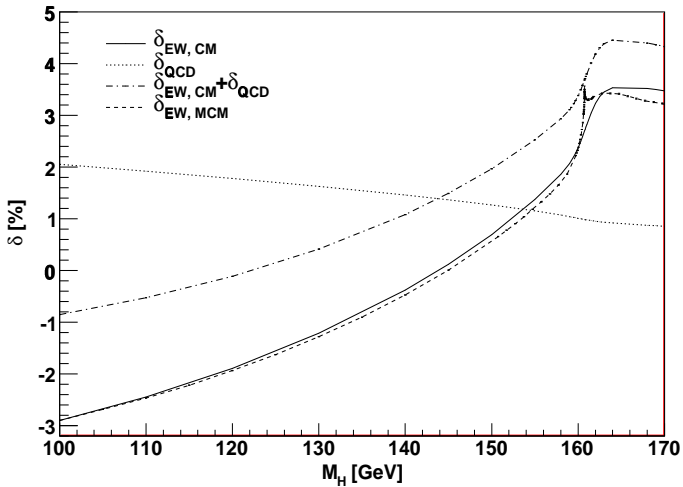
- In the full CM setup, the real parts of the W and Z self-energies induced by one-loop renormalization of the masses and the couplings have to be traded for the associated complex expressions.



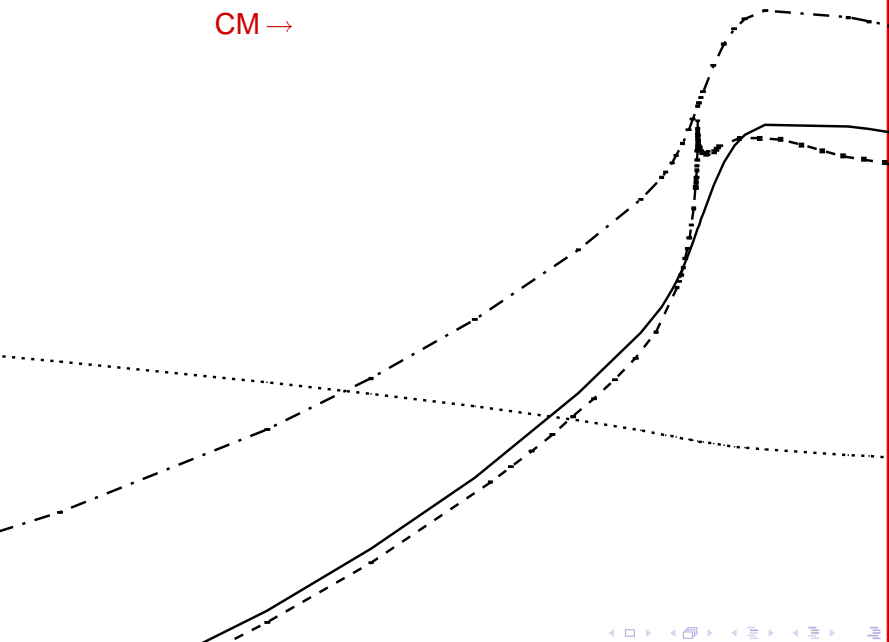
EW on gluon-gluon fusion



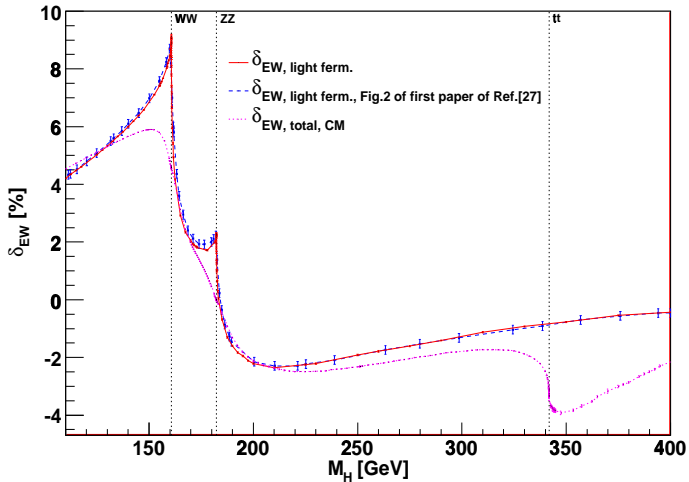
EW on decay ($\gamma\gamma$)

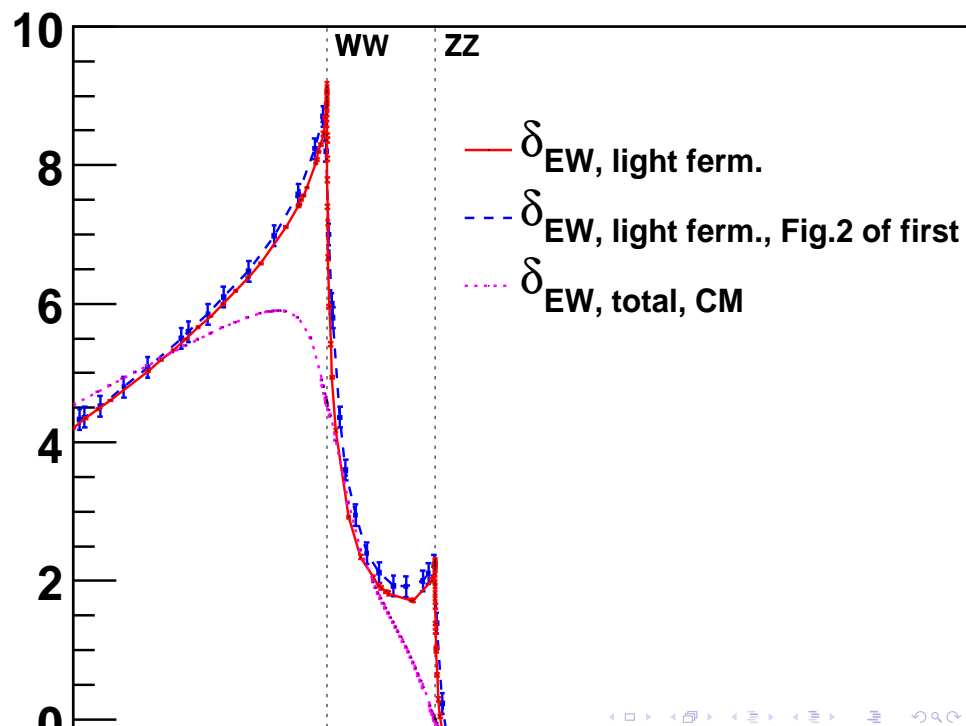


CM →

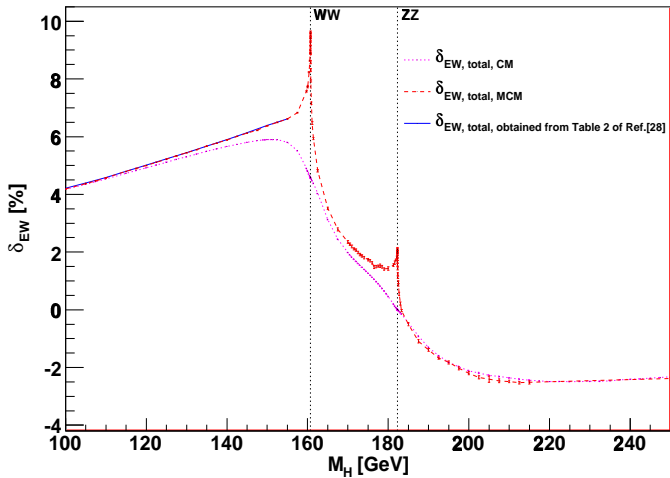


Comparing



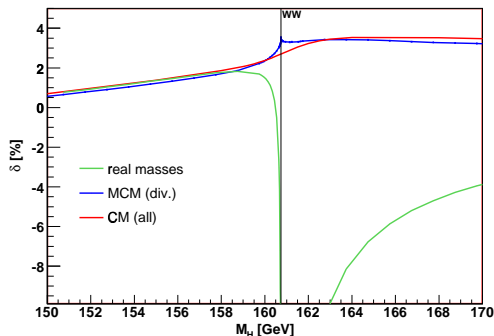


Comparing



Threshold behaviour for $H \rightarrow \gamma\gamma$

Comparison of EW corrections to $H \rightarrow \gamma\gamma$ around the WW threshold, obtained using **different schemes** for treating unstable particles



- Result obtained with real masses divergent at WW ; good approx. below; completely off above threshold, since no cancellation mechanism occurs
- Result in MCM setup finite, shows cusp; result in CM setup is smooth
- At threshold, result in MCM setup $\rightarrow 3.5\%$; result in CM setup $\rightarrow 2.7\%$
 \Rightarrow prediction at the % level requires complete CMS implementation

EW on K-factors - uncertainty

We introduce two **options** for including NLO electroweak corrections

- CF (Complete Factorization):

$$\sigma^{(0)} \mathbf{G}_{ij} \rightarrow \sigma^{(0)} \left(1 + \delta_{\text{EW}}(M_H^2) \right) \mathbf{G}_{ij};$$

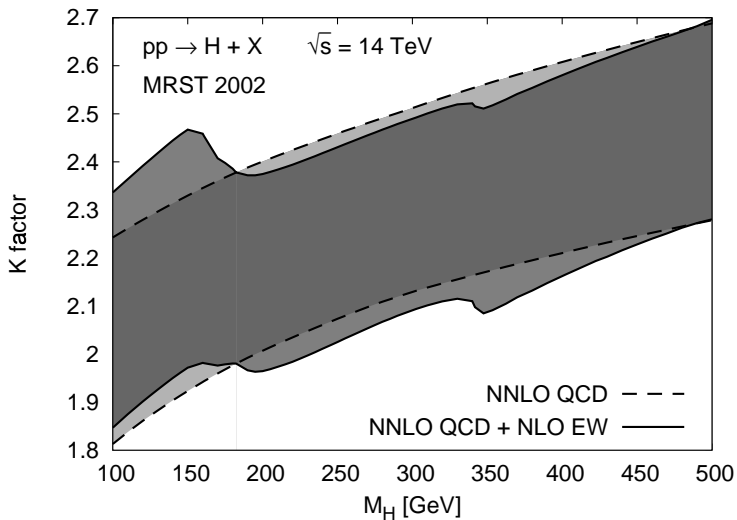
- PF (Partial Factorization):

$$\sigma^{(0)} \mathbf{G}_{ij} \rightarrow \sigma^{(0)} \left[\mathbf{G}_{ij} + \alpha_S^2(\mu_R^2) \delta_{\text{EW}}(M_H^2) \mathbf{G}_{ij}^{(0)} \right],$$

Can we do it better? Babis, Radja and Frank say yes



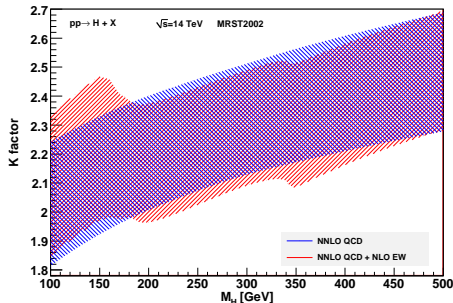
EW on K-factors - LHC



Result:

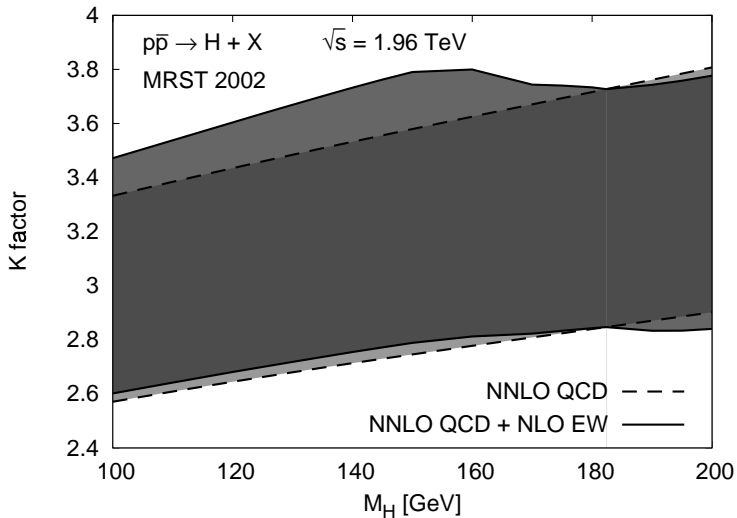
The hadronic process $pp \rightarrow H + X$

- Use Fortran program HiggsNNLO by **M. Grazzini**
- K-factor: Ratio cross section with higher orders over LO result



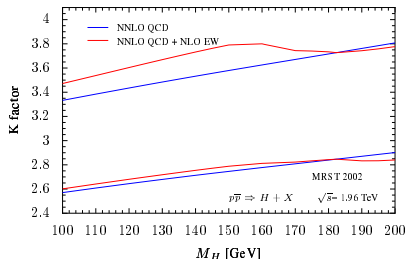
- Uncertainty band: Variation of μ_R , μ_F , PF, CF
- Central value for cross section is shifted by 2-5% ($M_H = 120$ GeV)

EW on K-factors - Tevatron



NLO EW corrections at the Tevatron

Impact of NLO EW effects at Tevatron II, $\sqrt{s} = 1.96$ TeV,
 $100 \text{ GeV} < M_H < 200 \text{ GeV}$ (using HIGGSNNLO, by M.Grazzini)

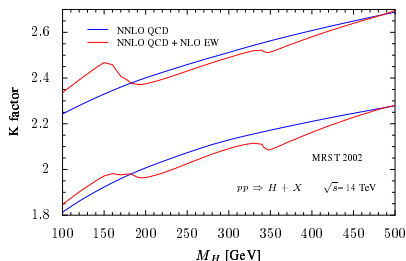


M_H [GeV]	δ_{CF} [%]	δ_{PF} [%]
120	+4.9	+1.6
140	+5.7	+1.8
160	+4.8	+1.5
180	+0.5	+0.1
200	-2.1	-0.6

- Uncertainty band shows stronger sensitivity on the Higgs mass, once NLO EW effects are included
- Impact of NLO EW corrections smaller respect to NNLL resummation
 Catani, de Florian, Grazzini, Nason'03 (+12% for $M_H = 120$ GeV)
- 95% CL exclusion of a SM Higgs for $M_H = 170$ GeV, % effects relevant;
 CM result employed by Anastasiou, Boughezal, Petriello'08,
 prediction σ is 7 – 10% larger than σ used by TEVNPH WG

NLO EW corrections at the LHC

Impact of NLO EW effects at LHC, $\sqrt{s} = 14$ TeV,
 $100 \text{ GeV} < M_H < 500 \text{ GeV}$ (using HIGGSNNLO, by M.Grazzini)



M_H [GeV]	δ_{CF} [%]	δ_{PF} [%]
120	+4.9	+2.4
150	+5.9	+2.8
200	-2.1	-1.0
310	-1.7	-0.9
410	-0.8	-0.8

- Uncertainty band shows stronger sensitivity on the Higgs mass, once NLO EW effects are included
- WW and $t\bar{t}$ thresholds visible, but smooth having introduced everywhere CMs
- Impact of NLO EW corrections comparable to that of NNLL resummation [Catani, de Florian, Grazzini, Nason'03](#) (+6% for $M_H = 120$ GeV); for large M_H NLO EW corrections turn negative, screening effect with NNLL resummation